## 3. DISTRIBUTIONS OF ENVELOPE LEVEL CROSSINGS

The analyses of the first-order statistics of the noise/interference that were discussed in Part I, as well as the autocorrelation functions discussed above, provide support for modeling the noise/interference as a combination of Gaussian noise, narrowband interferers (sine waves), and impulsive noise (train of impulses). Comparisons of measured and simulated cumulative distributions of power in the time and frequency domains indicate that modeling the amplitude distributions of the sine waves and impulses as Hall distributions is approximately correct. The variety of time domain waveforms and power spectra suggests treating the frequencies of the sine waves as a random variable; a uniform distribution for this random variable is simple and appears to be consistent with the measured data. Furthermore, it seems reasonable to treat the phases of the sine waves as a uniformly distributed random variable, since the different sine waves presumably arise from independent sources. However, it remains to investigate the distribution of the times of arrival of the impulses.

Impulsive noise from man-made sources may be correlated in time, due to machinery which generates noise bursts in a repetitive fashion. Inspection of the time domain waveforms with impulsive noise (case study 5) reveals a tendency for the impulses to occur periodically in time. However, the impulses are not precisely periodic in time, and, as discussed above, this is corroborated by the absence of periodic impulses in the autocorrelation function. Moreover, it is well-known that the impulses in atmospheric noise are clustered in time, due to the presence of numerous individual strokes in a single lightning burst (Uman, 1987). It would therefore be incorrect to model the times of arrival of the impulses either as periodic or as a uniformly distributed random variable.

Further insight concerning the arrival times of the impulses can be gained by investigating the distributions of level crossings of the noise/interference envelope. These distributions provide information about the widths and spacings of the impulses. The calculation of these distributions is difficult, requiring numerical techniques even for the case of Gaussian processes (Rice, 1945; McFadden, 1956; Longuet-Higgins, 1962). Therefore, no attempt will be made to obtain analytic expressions for these distributions in the noise/interference model, as was done for the autocorrelation function. Instead, a purely empirical approach will be adopted, whereby the

distributions computed from the measured data will be qualitatively compared with those from the simulated data, with the goal of refining the model to make the measured and simulated distributions consistent with one another.

### 3.1 Pulse Width and Pulse Spacing Distributions

Pulse width is defined as the time interval between an upgoing crossing of the voltage envelope ($\sqrt{(I^2+Q^2)}$) through some threshold and the next downgoing crossing of the envelope through that same threshold. Conversely, pulse spacing is defined as the time interval between a downgoing crossing of the envelope through some threshold and the next upgoing crossing through that threshold. Thus, for a given data record, a family of distributions (corresponding to various thresholds) is required to characterize the distributions of pulse widths and pulse spacings. Accordingly, sets of distributions have been computed for each of the five case studies. As a point of reference, the first 4 ms of the voltage envelope have also been plotted for each of the case studies, so that one can make a correspondence between the values of the thresholds that were chosen and the structure of the voltage envelope.

The results are shown in Figures 23 through 37. The pulse width and spacing distributions have been presented in the form of plots in which each point corresponds to the number of occurrences of a pulse width (spacing) of a given time duration. To obtain a sufficient number of occurrences to clearly reveal the trends in the distributions, it was necessary to analyze the entire one-second record for each of the cases. The distributions corresponding to different thresholds have been plotted on separate scales for clarity; however, to facilitate comparisons, the scales of the different plots in each figure are the same. These scales were chosen to be logarithmic, due to the large ranges of values that were encountered. Thus, the logarithm of the number of occurrences of a pulse width (spacing) of a given duration has been plotted versus the logarithm of that duration in microseconds.

Although no analytical results have been derived with which to compare the measured distributions, the qualitative behavior of the distributions is in accord with intuition. For example, the voltage envelope equals zero if and only if the I- and Q-channel voltages simultaneously equal zero, which is a relatively rare event. Therefore, the voltage envelope vanishing at two or more consecutive sample times is an extremely rare event. Thus, at zero

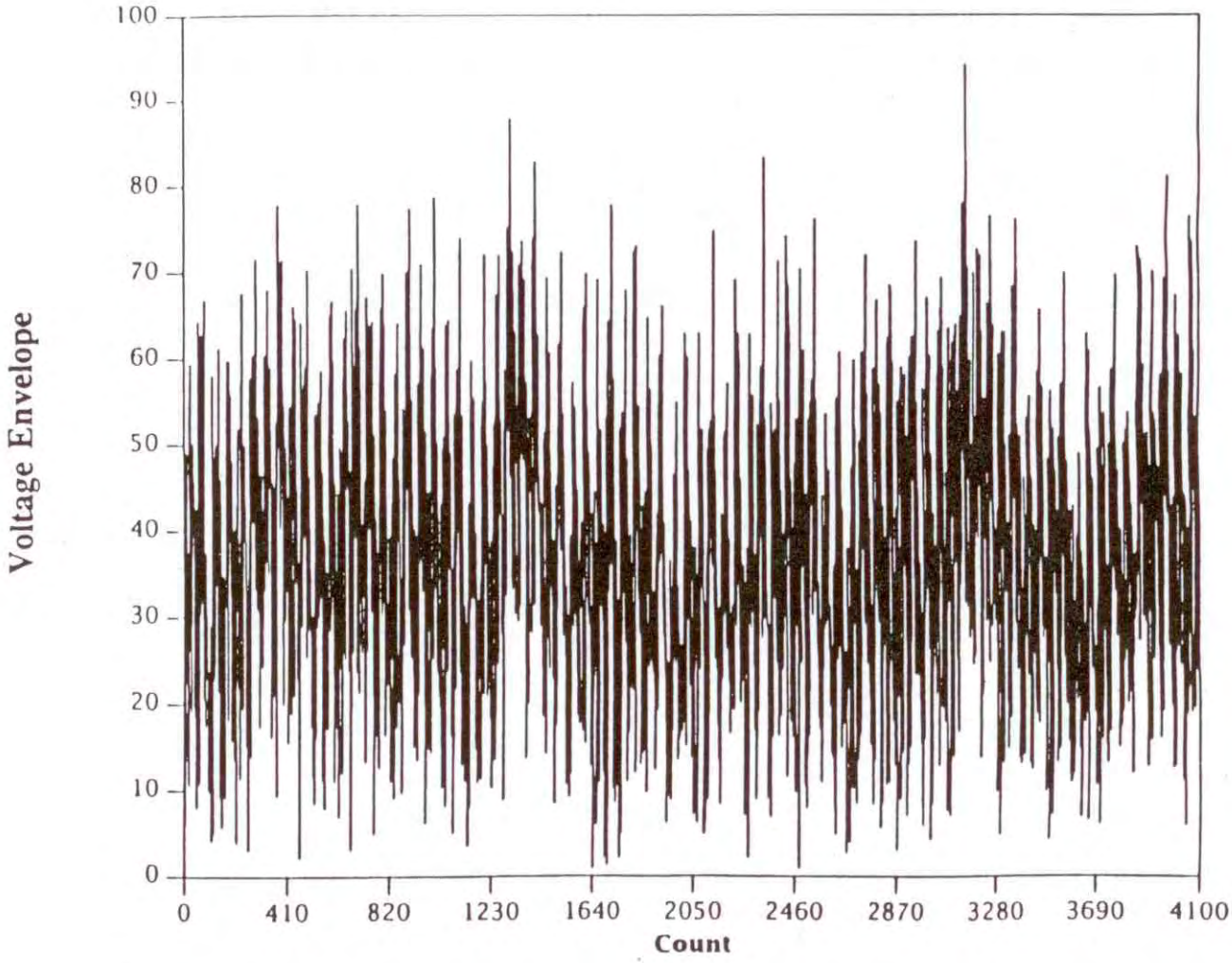


Figure 23. Voltage envelope of measured noise/interference (case study 1).

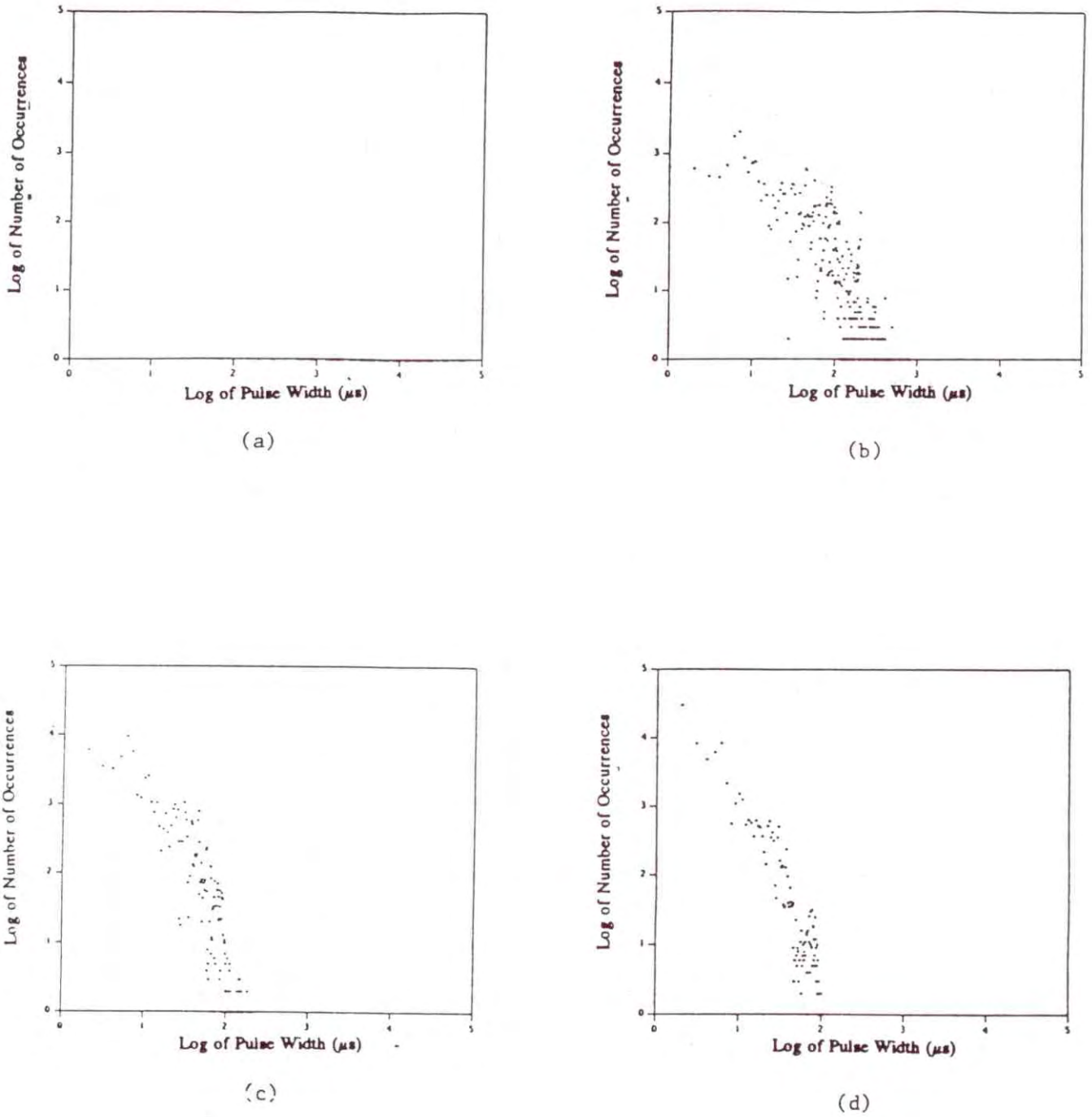


Figure 24. Pulse width distributions of measured noise/interference at thresholds of (a) 0, (b) 10, (c) 20, (d) 30, (e) 40, (f) 50, (g) 70, and (h) 90 (case study 1).

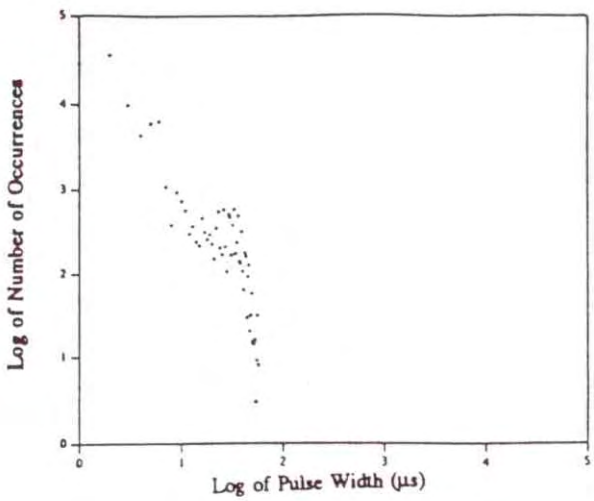


(e)

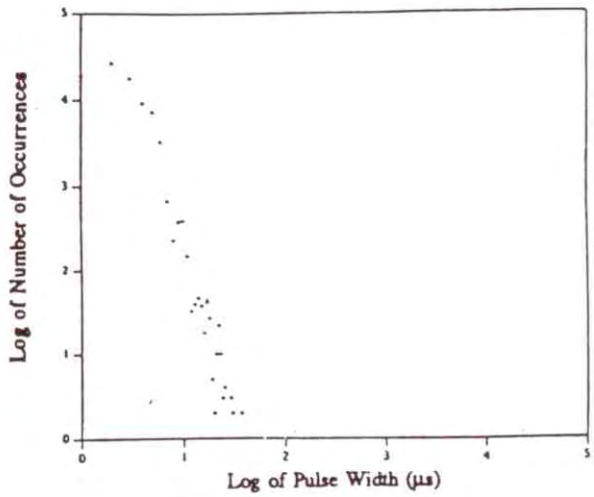


(f)

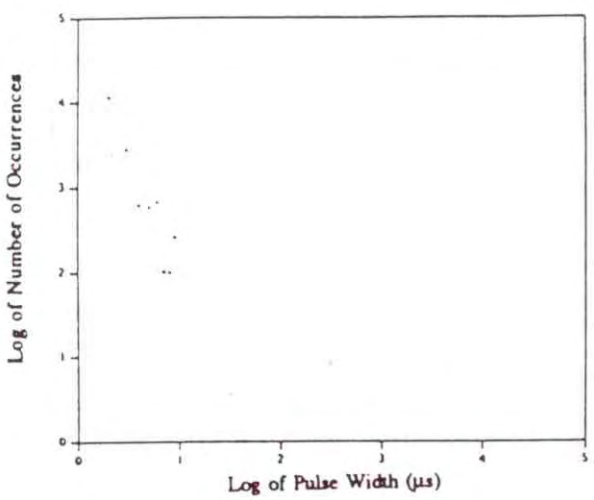


(g)

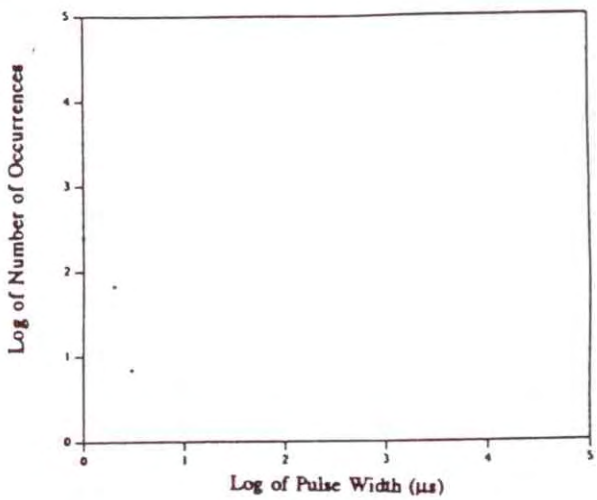


(h)

Figure 24 (cont.). Pulse width distributions of measured noise/interference at thresholds of (a) 0, (b) 10, (c) 20, (d) 30, (e) 40, (f) 50, (g) 70, and (h) 90 (case study 1).

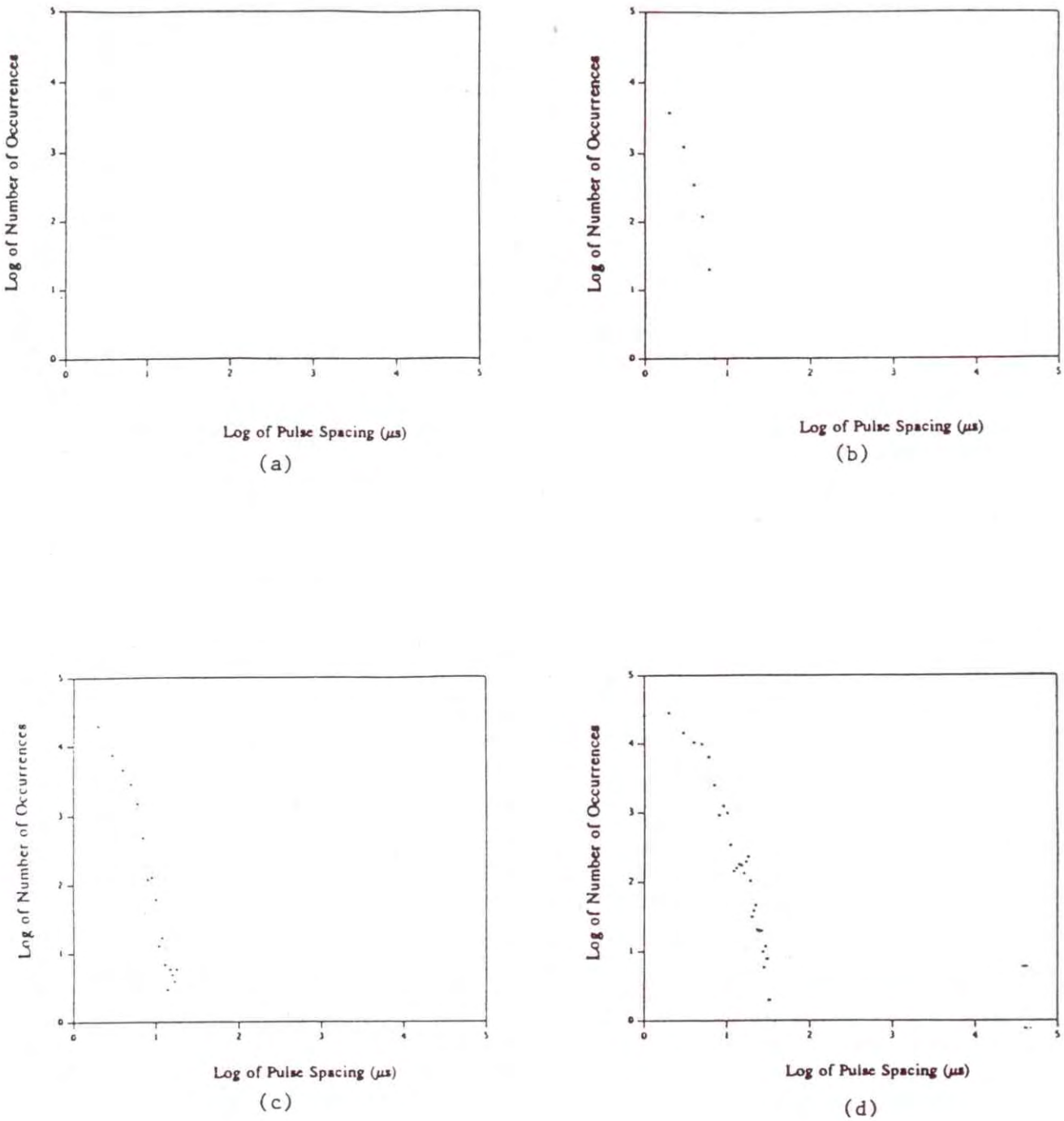


Figure 25. Pulse spacing distributions of measured noise/interference at thresholds of (a) 0, (b) 10, (c) 20, (d) 30, (e) 40, (f) 50, (g) 70, and (h) 90 (case study 1).

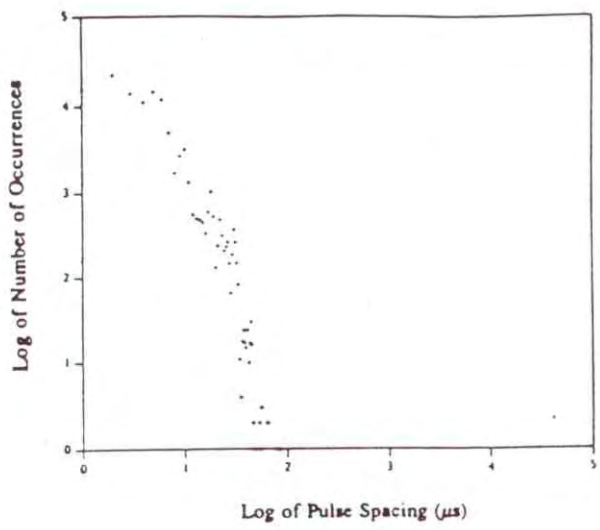


(e)

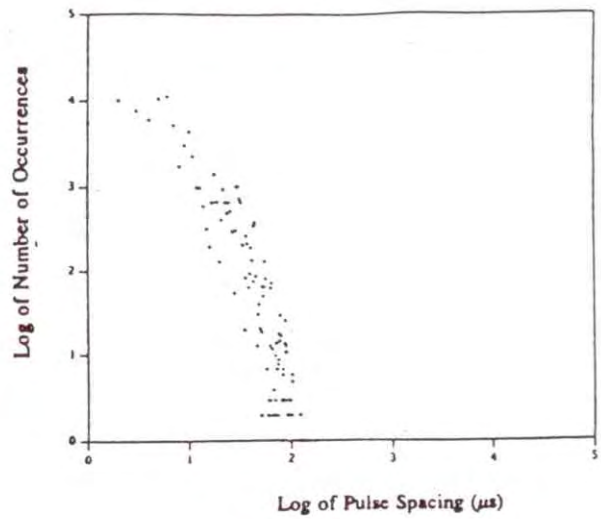


(f)

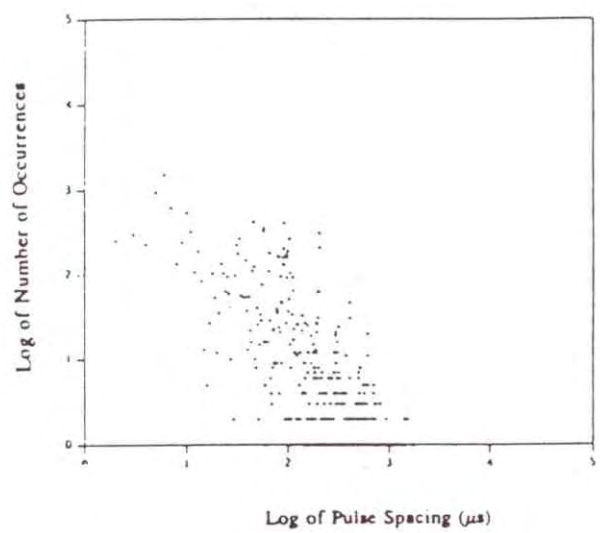


(g)

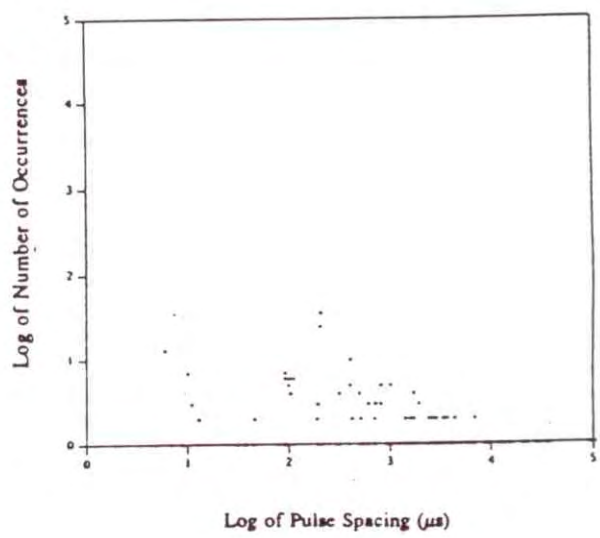


(h)

Figure 25 (cont.). Pulse spacing distributions of measured noise/interference at thresholds of (a) 0, (b) 10, (c) 20, (d) 30, (e) 40, (f) 50, (g) 70, and (h) 90 (case study 1).

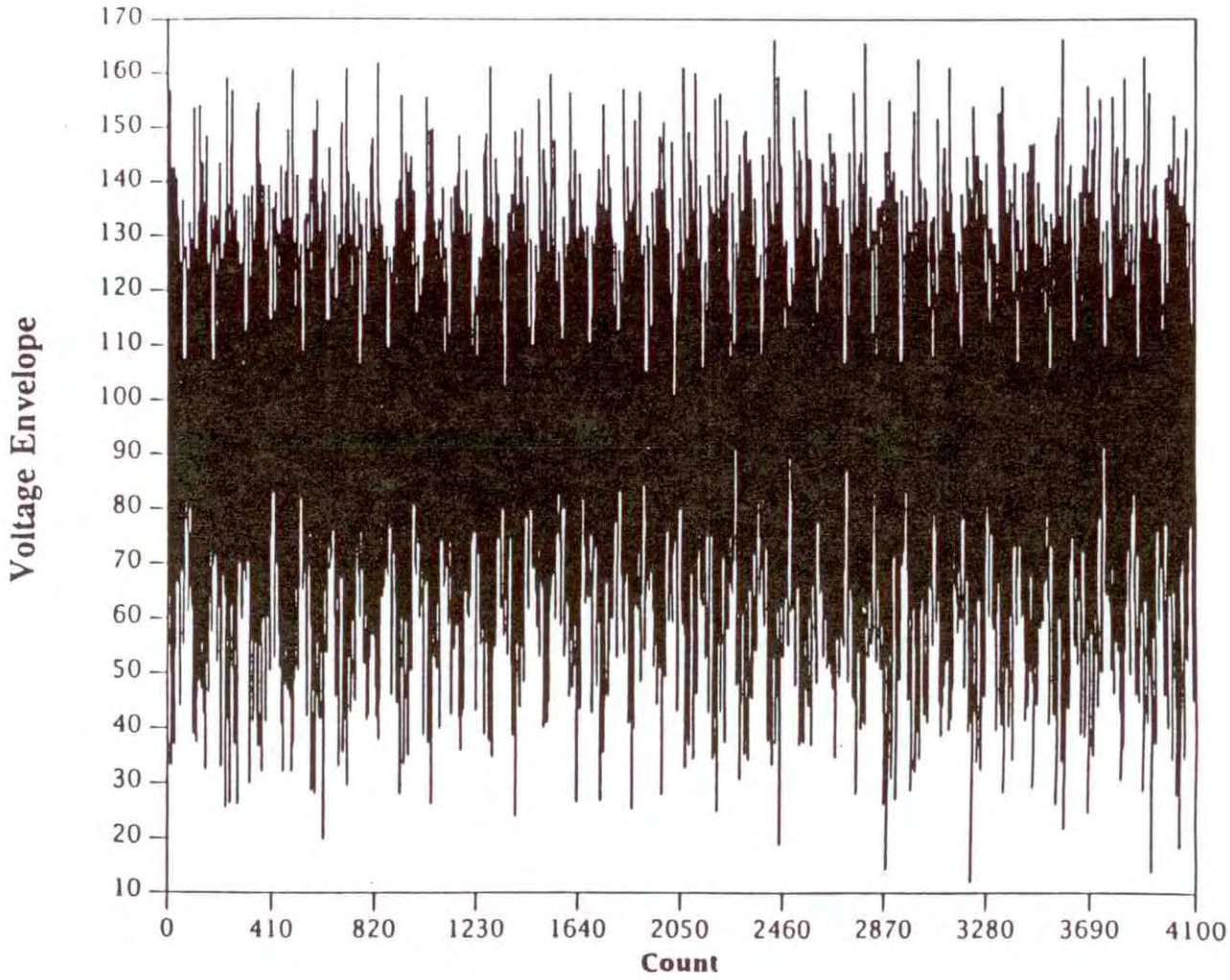


Figure 26. Voltage envelope of measured noise/interference (case study 2).

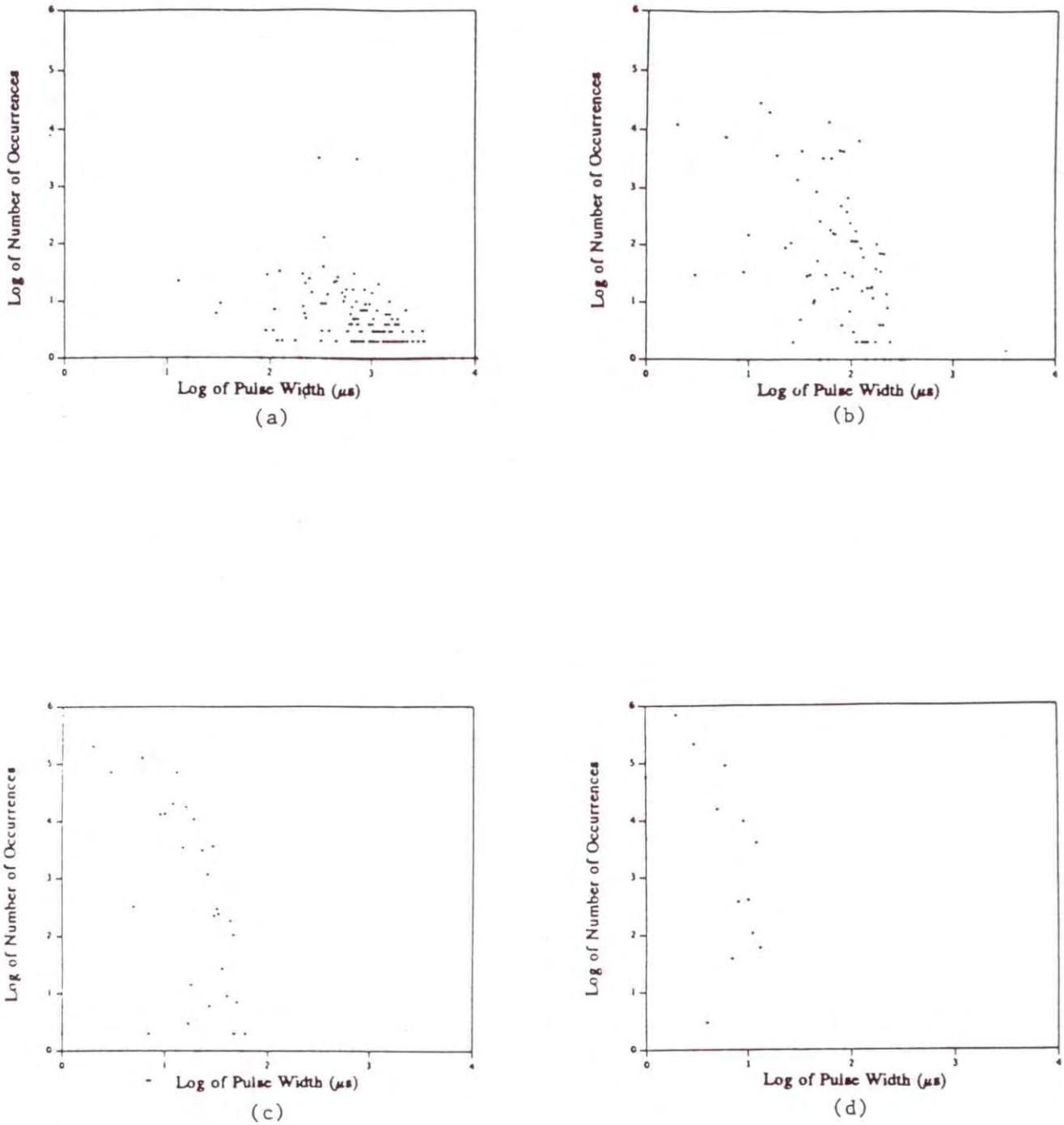


Figure 27. Pulse width distributions of measured noise/interference at thresholds of (a) 20, (b) 40, (c) 60, (d) 80, (e) 100, (f) 120, (g) 140, (h) 160 (case study 2).

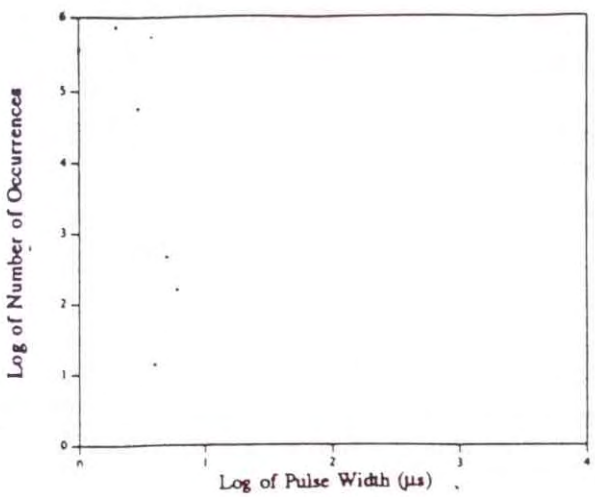


(e)

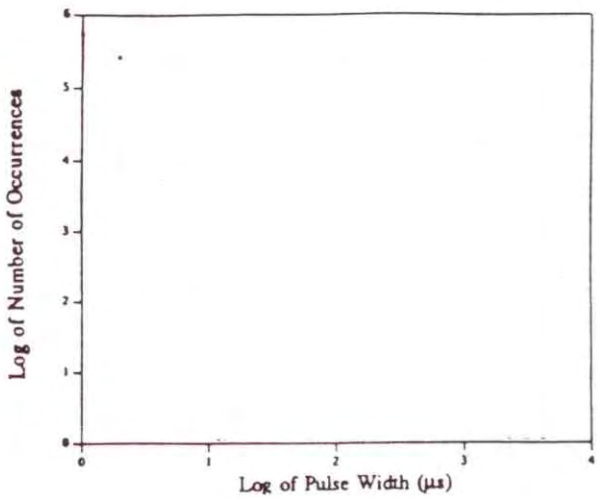


(f)

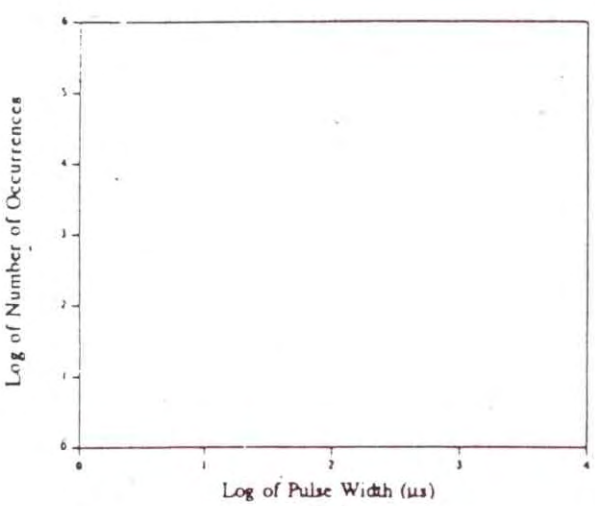


(g)

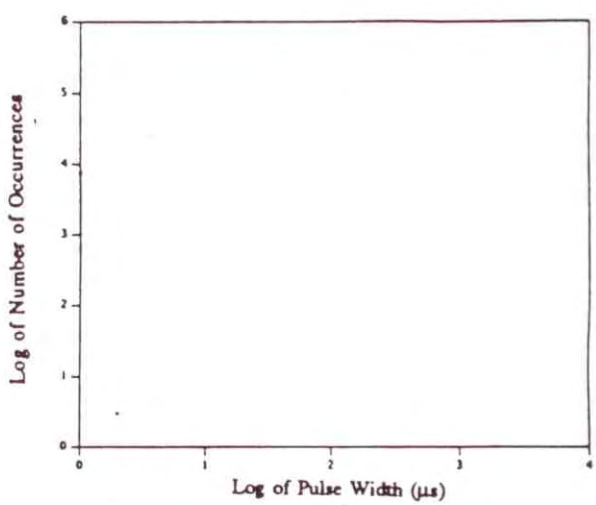


(h)

Figure 27 (cont.). Pulse width distributions of measured noise/interference at thresholds of (a) 20, (b) 40, (c) 60, (d) 80, (e) 100, (f) 120, (g) 140, (h) 160 (case study 2).

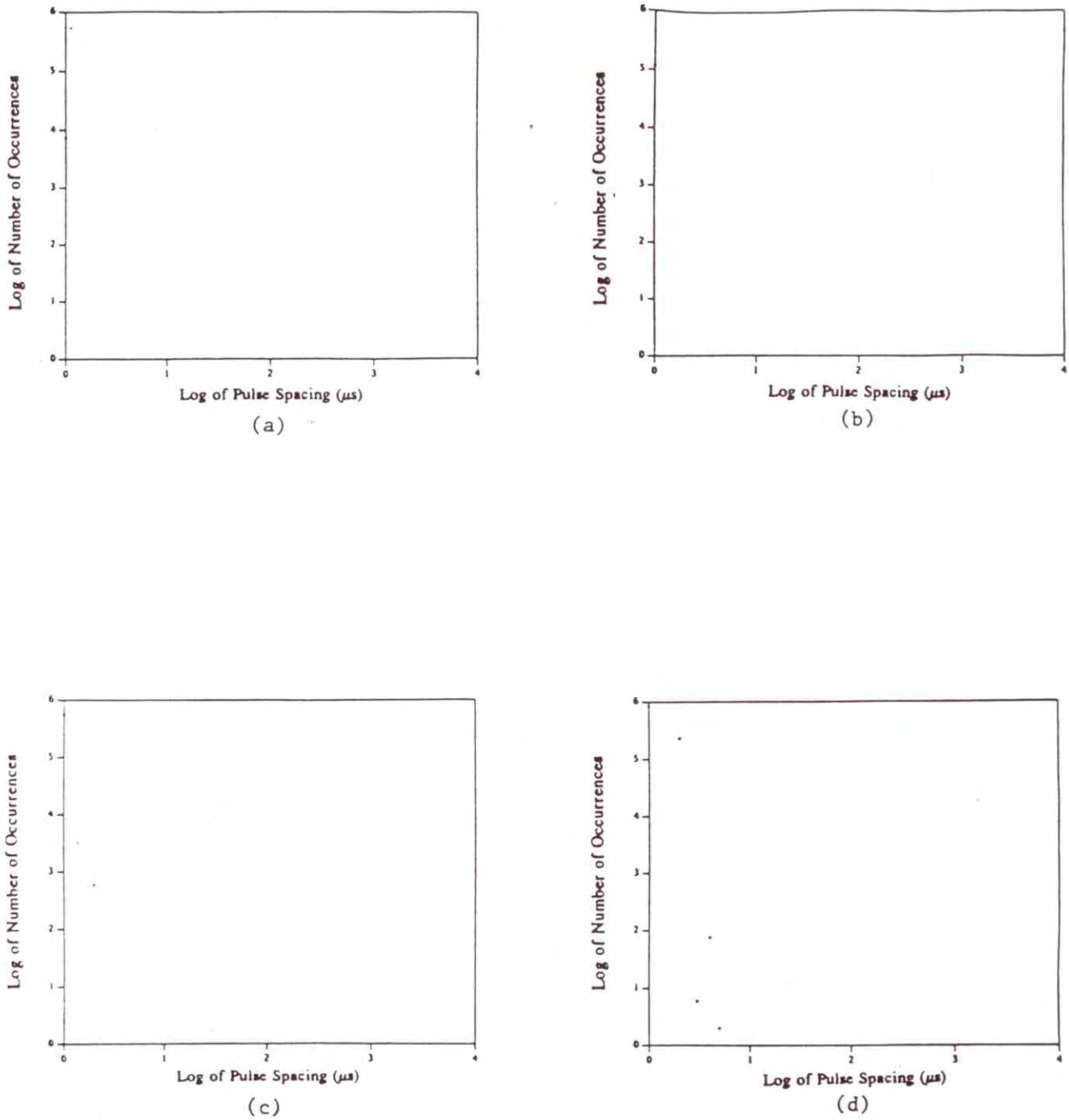


Figure 28. Pulse spacing distributions of measured noise/interference at thresholds of (a) 20, (b) 40, (c) 60, (d) 80, (e) 100, (f) 120, (g) 140, and (h) 160 (case study 2).

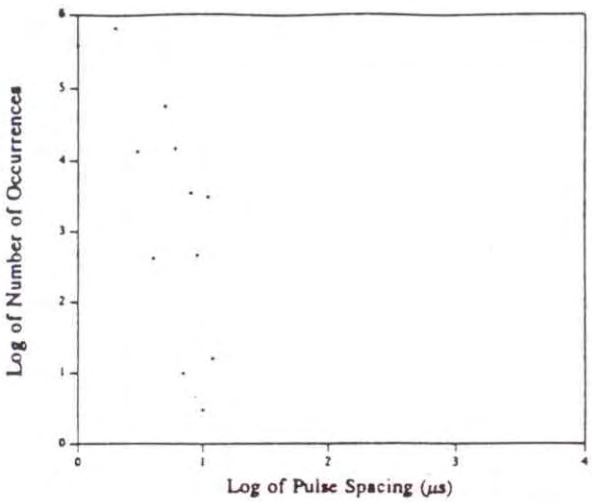


(e)

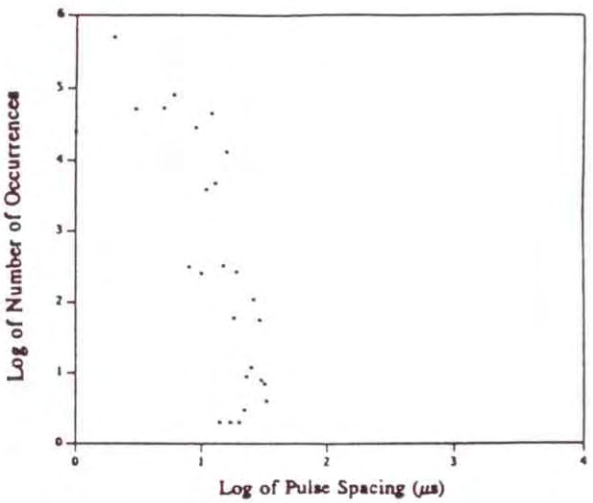


(f)

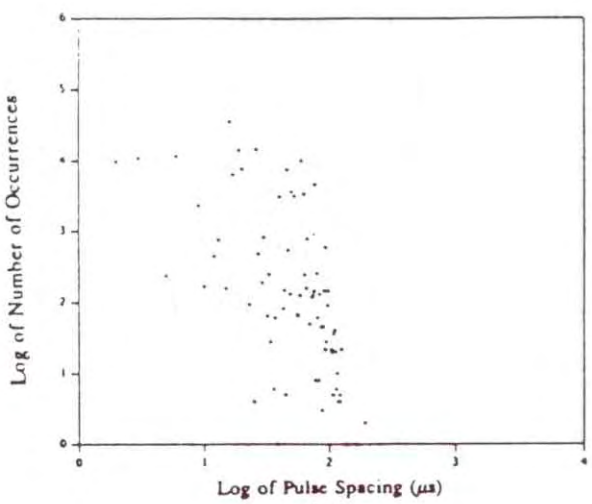


(g)

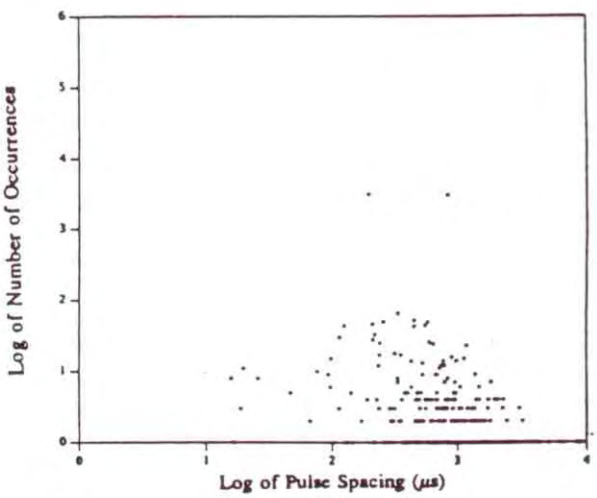


(h)

Figure 28 (cont.). Pulse spacing distributions of measured noise/interference at thresholds of (a) 20, (b) 40, (c) 60, (d) 80, (e) 100, (f) 120, (g) 140, and (h) 160 (case study 2).

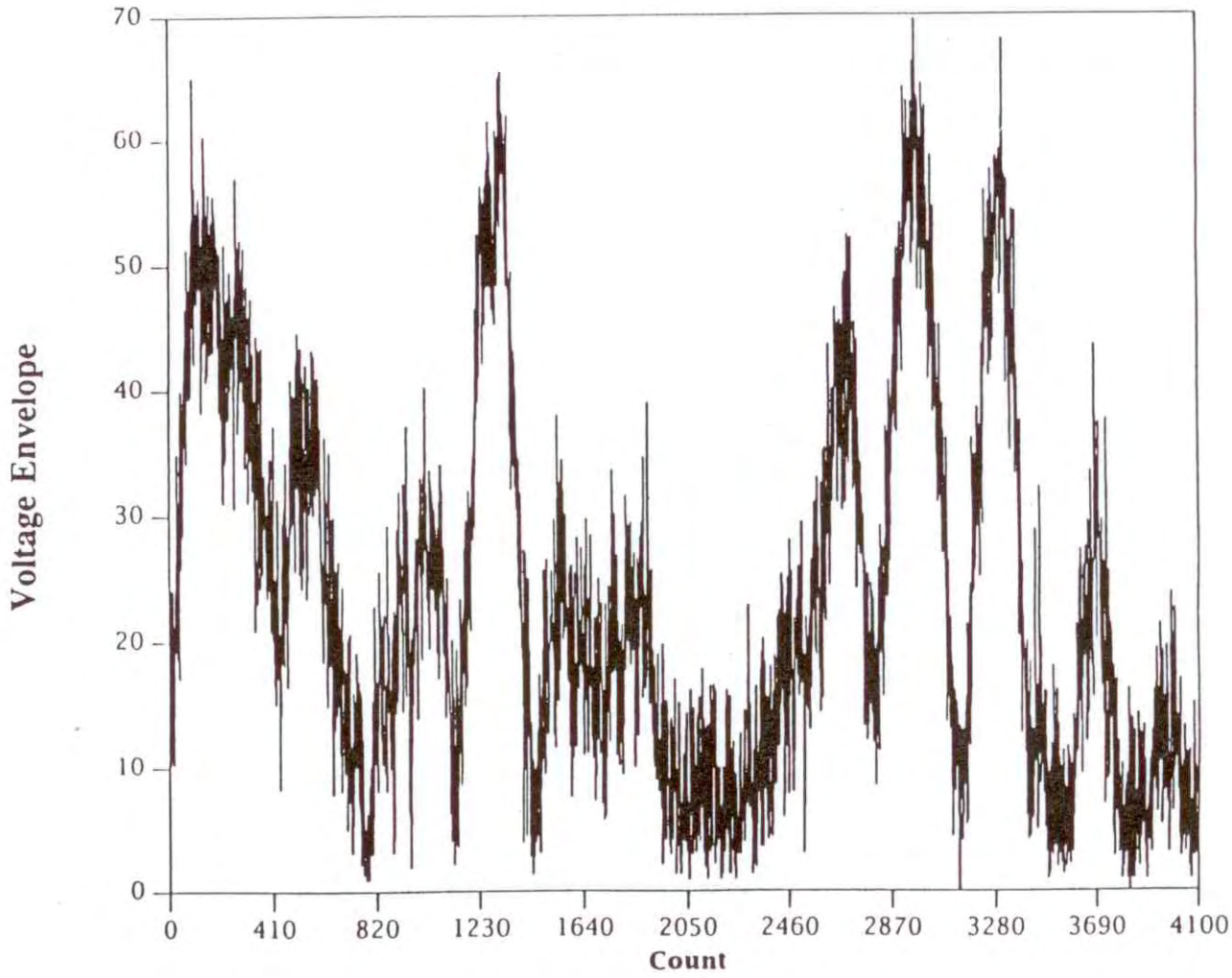


Figure 29. Voltage envelope of measured noise/interference (case study 3).

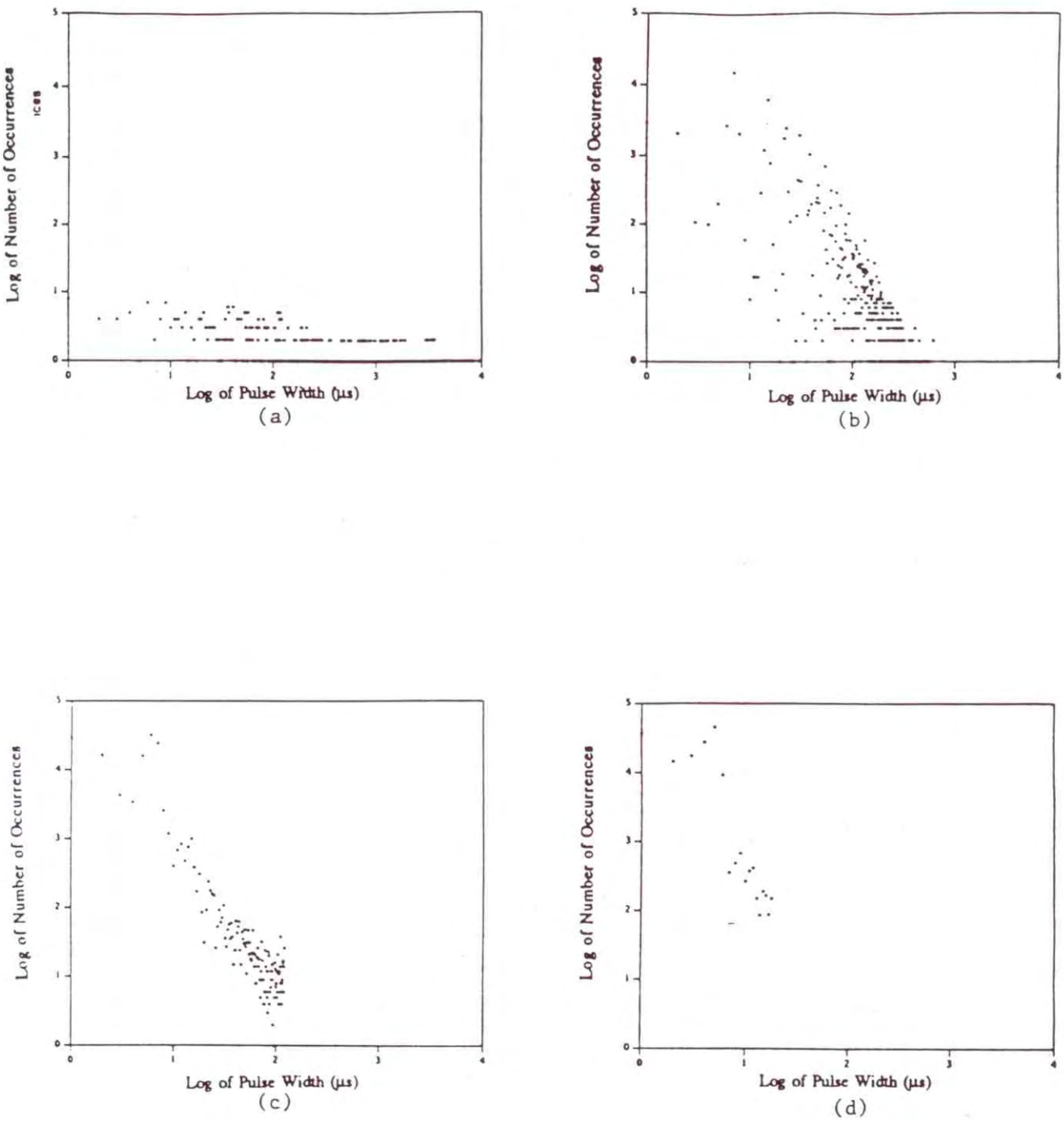


Figure 30. Pulse width distribution of measured noise/interference at thresholds of (a) 0, (b) 10, (c) 20, (d) 30, (e) 40, (f) 45 (case study 3).

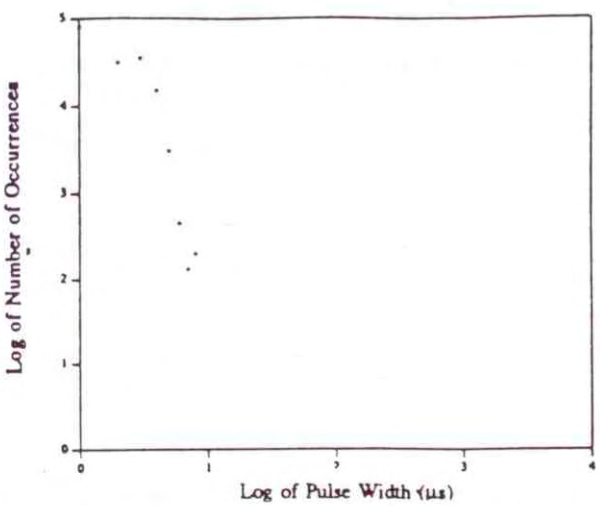


(e)

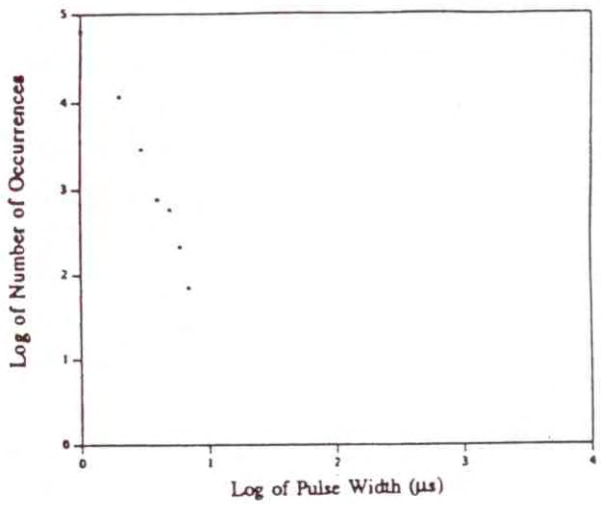


(f)

Figure 30 (cont.). Pulse width distributions of measured noise/interference at thresholds of (a) 0, (b) 10, (c) 20, (d) 30, (e) 40, (f) 45 (case study 3).

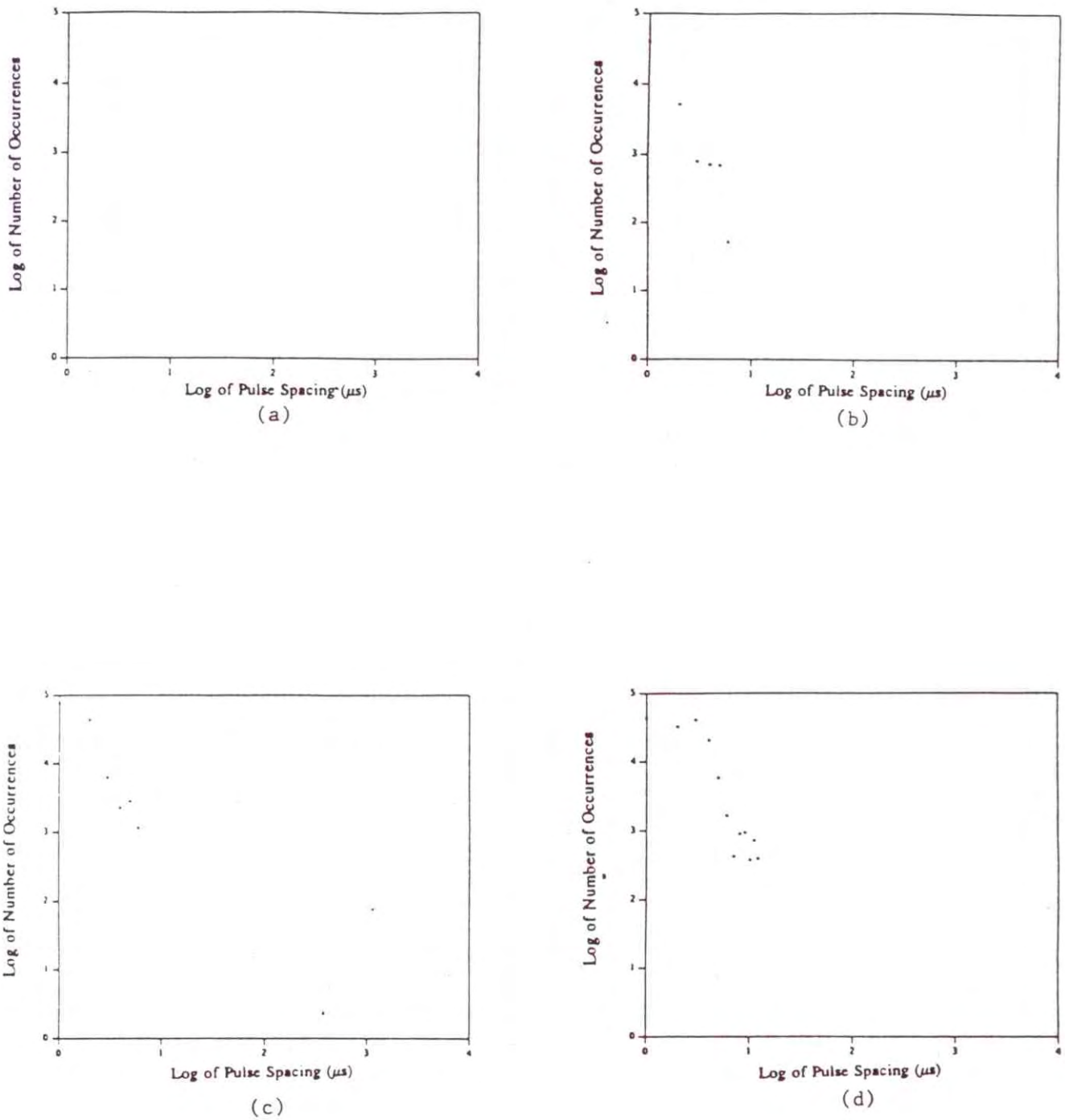


Figure 31. Pulse spacing distribution of measured noise/interference at thresholds of (a) 0, (b) 10, (c) 20, (d) 30, (e) 40, (f) 45 (case study 3).

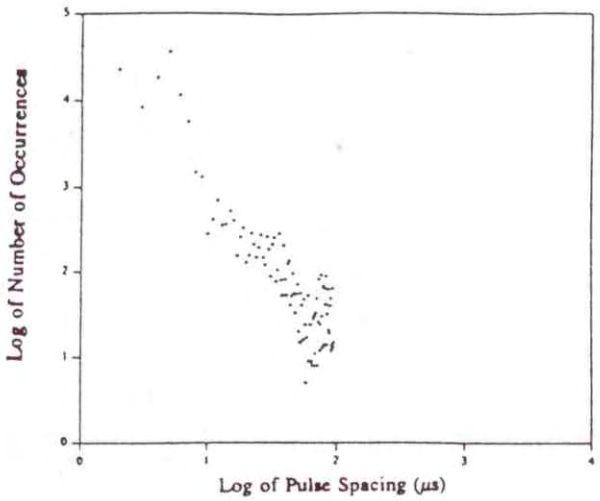


(e)

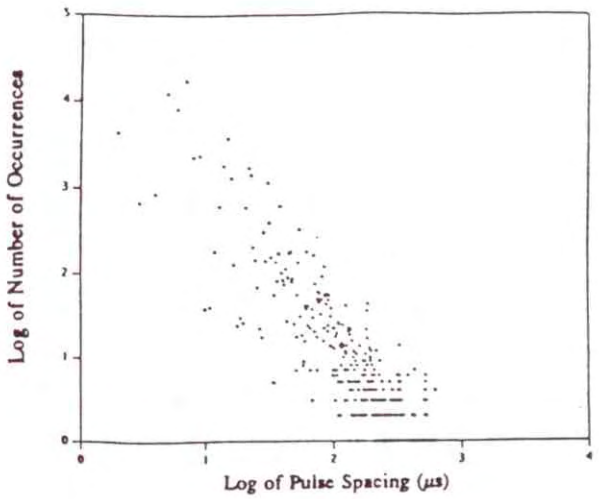


(f)

Figure 31 (cont.). Pulse spacing distribution of measured noise/interference at thresholds of (a) 0. (b) 10, (c) 20, (d) 30, (e) 40, (f) 45 (case study 3).

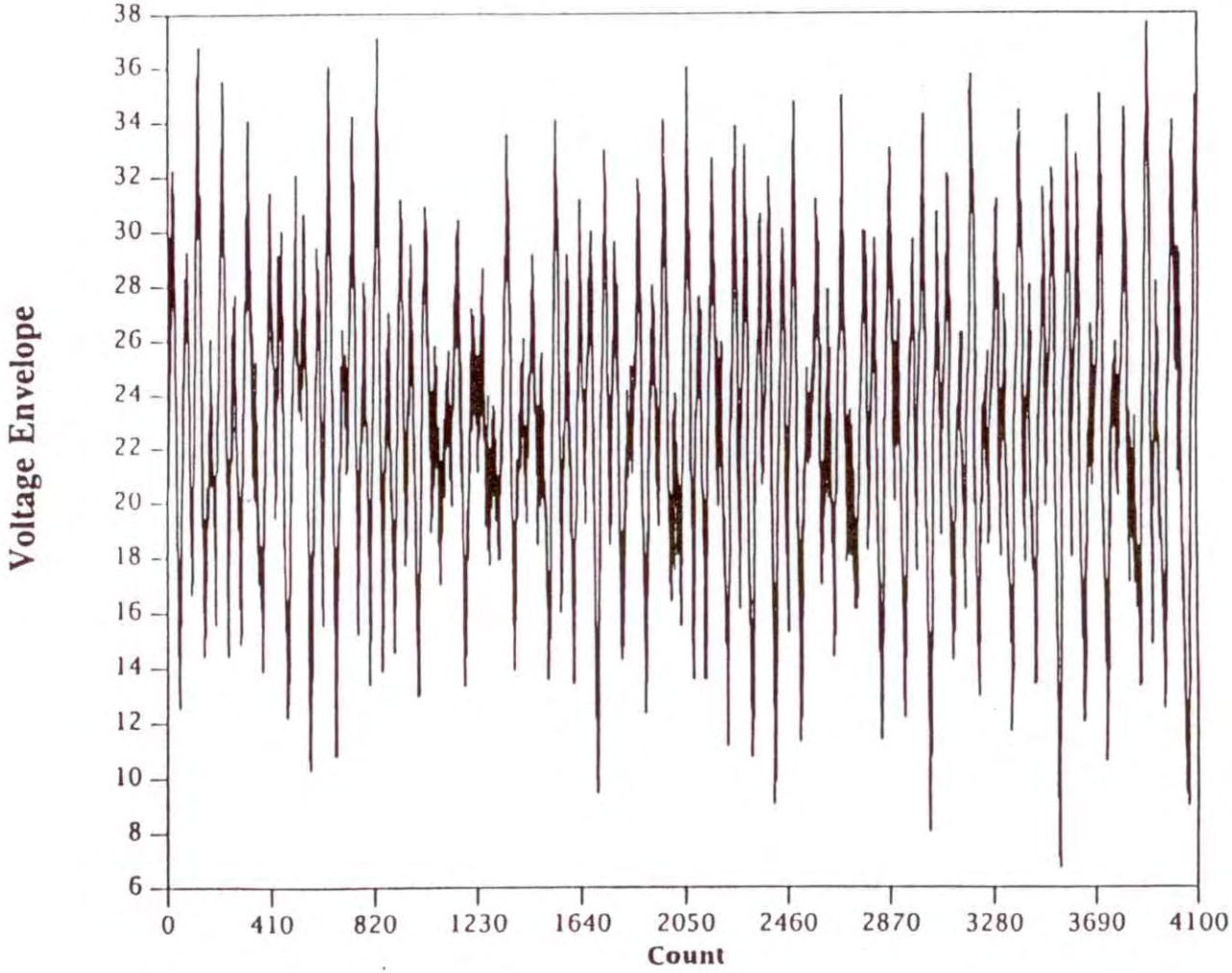


Figure 32. Voltage envelope of measured noise/interference (case study 4).

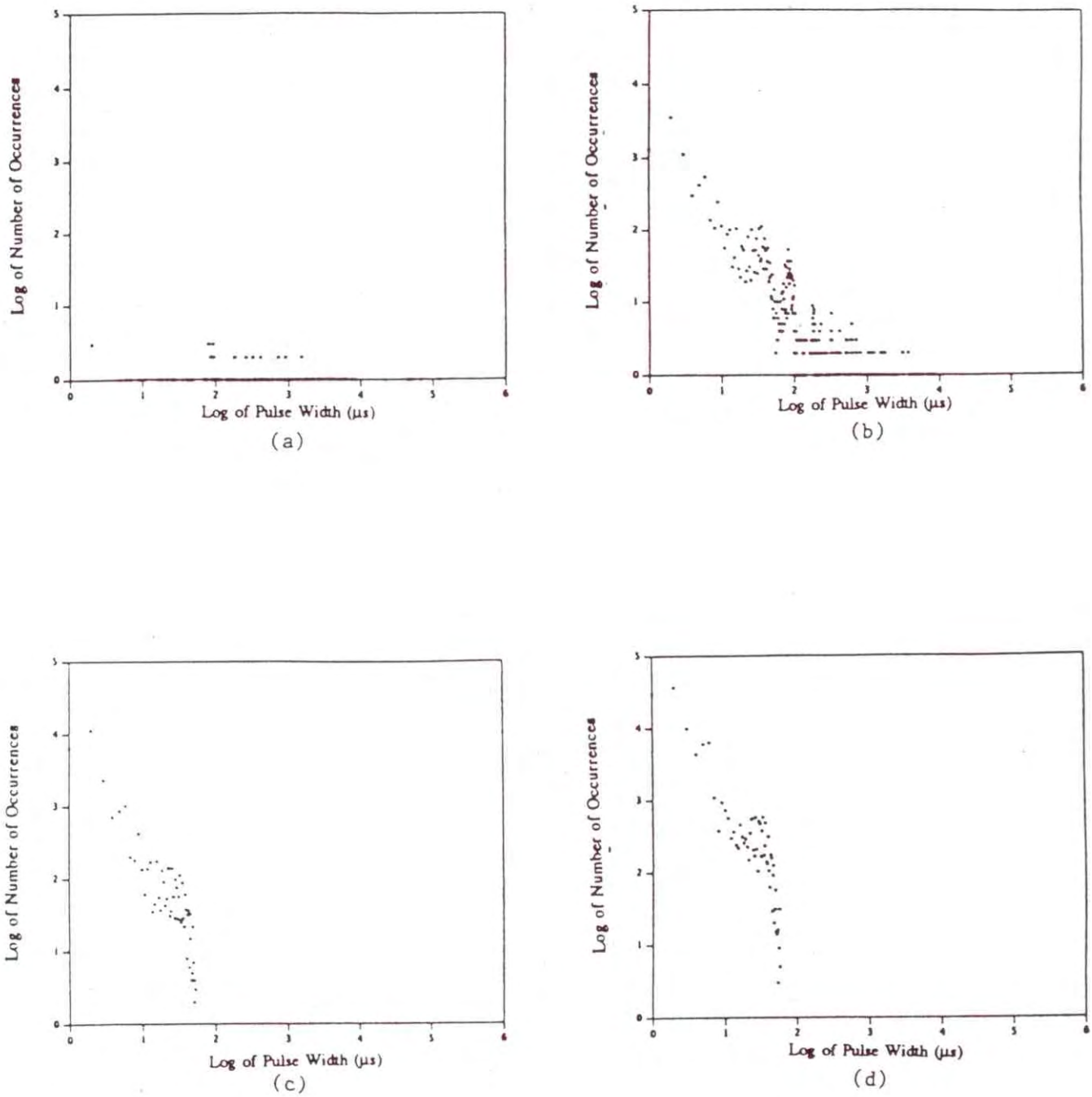


Figure 33. Pulse width distributions of measured noise/interference at thresholds of (a) 0, (b) 5, (c) 10, (d) 20, (e) 30, and (f) 40 (case study 4).

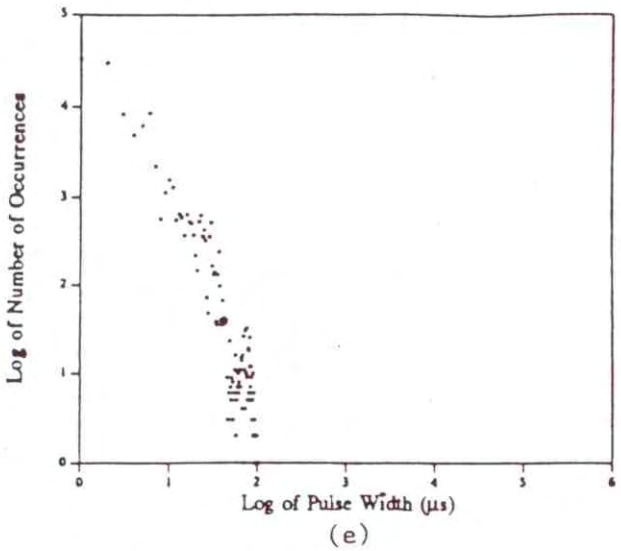


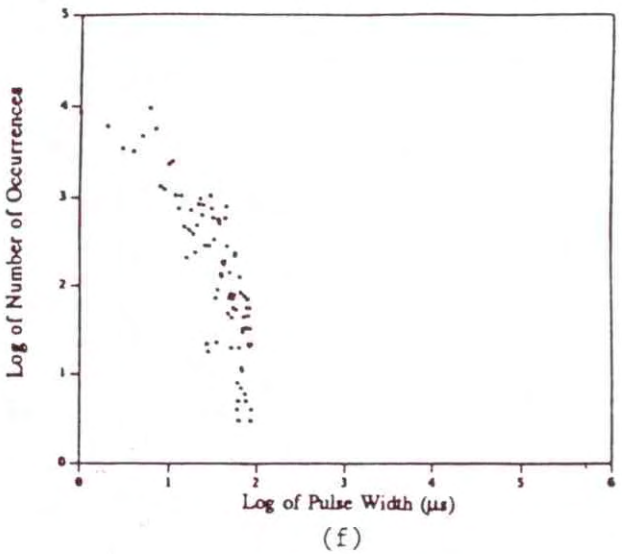


Figure 33 (cont.). Pulse width distributions of measured noise/interference at thresholds of (a) 0, (b) 5, (c) 10, (d) 20, (e) 30, and (f) 40 (case study 4).

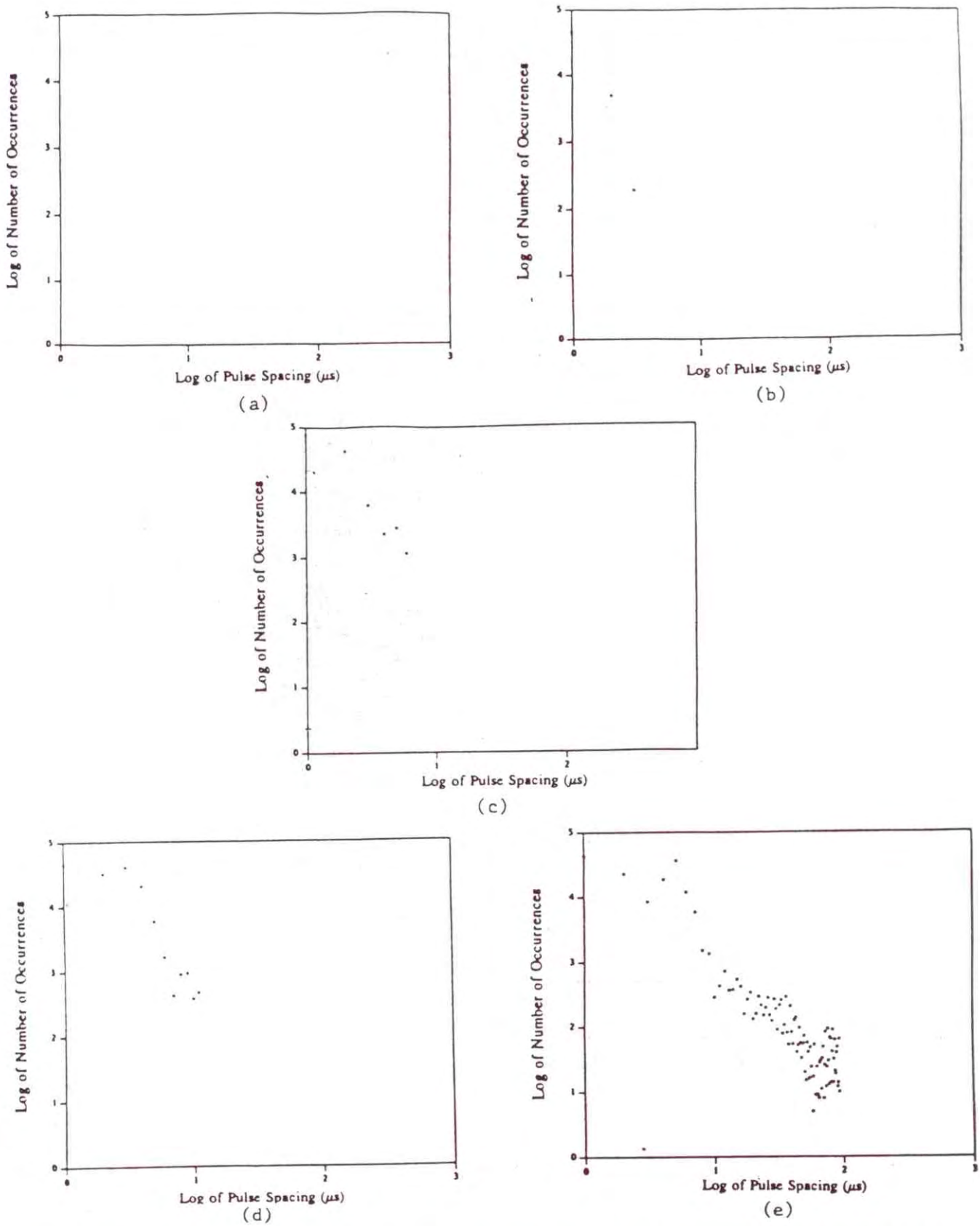


Figure 34. Pulse spacing distributions of measured noise/interference at thresholds of (a) 0, (b) 5, (c) 10, (d) 20, and (e) 30 (case study 4).

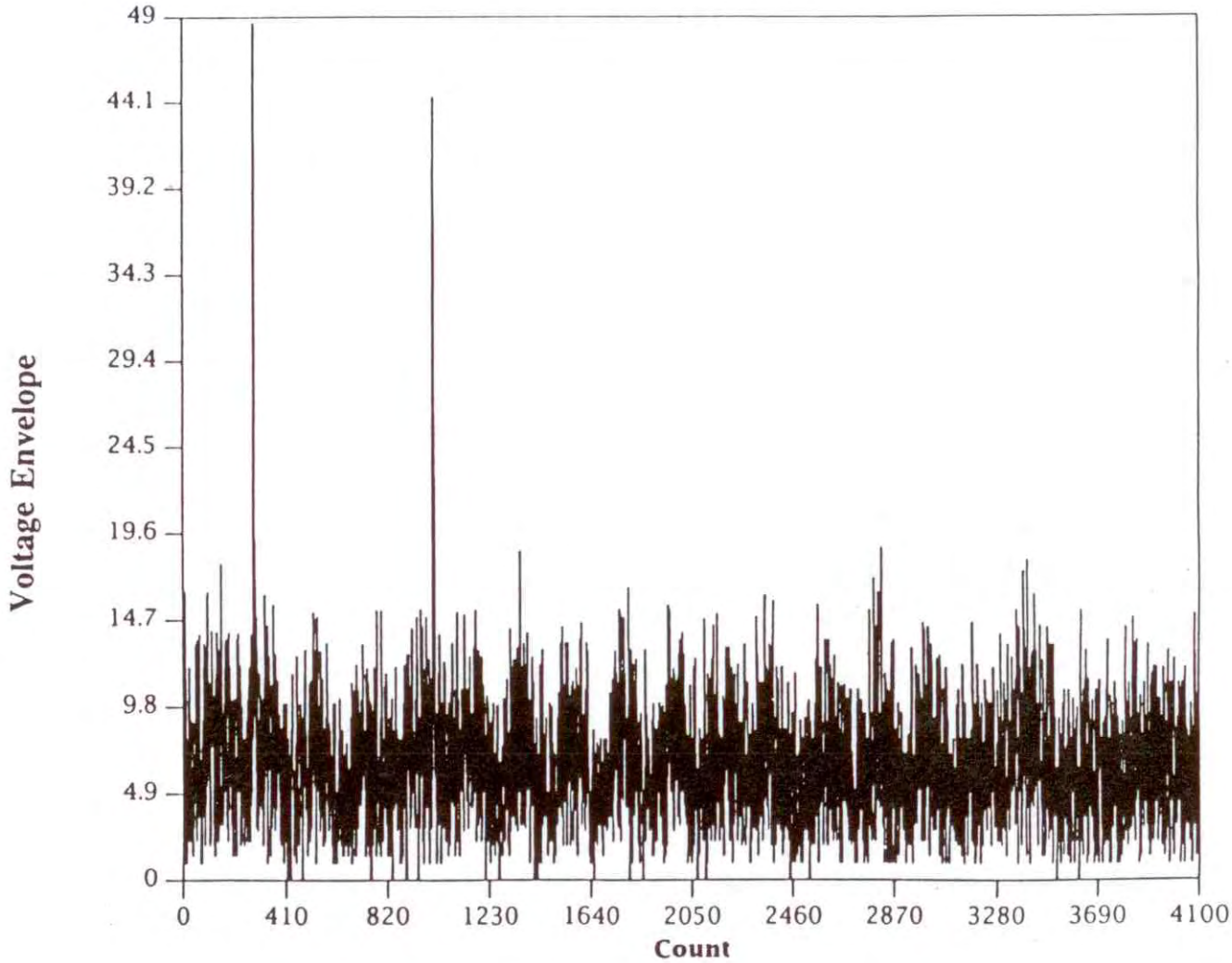


Figure 35. Voltage envelope of measured noise/interference (case study 5).

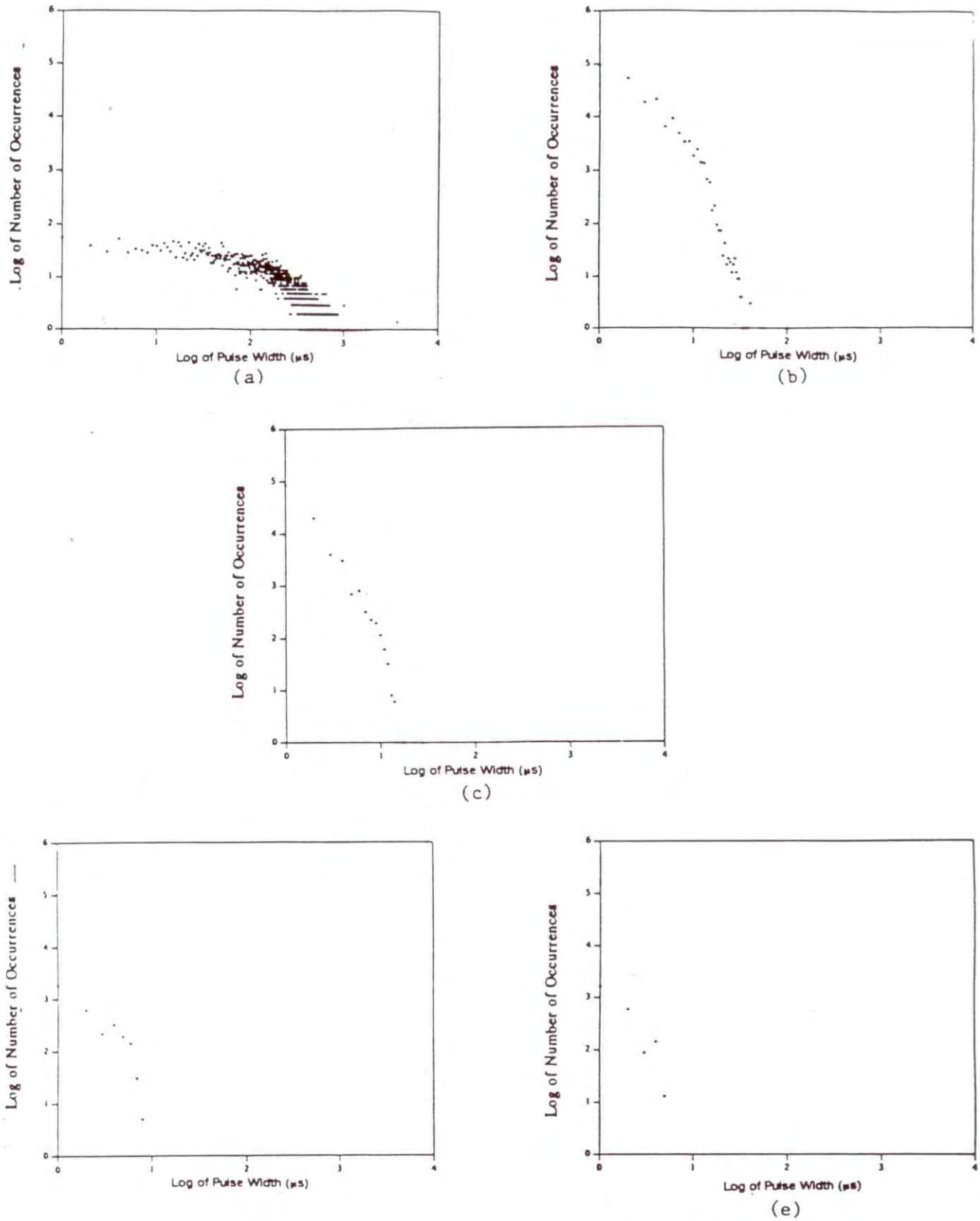


Figure 36. Pulse width distributions of measured noise/interference at thresholds of (a) 0, (b) 5, (c) 10, (d) 25, and (e) 30 (case study 5).

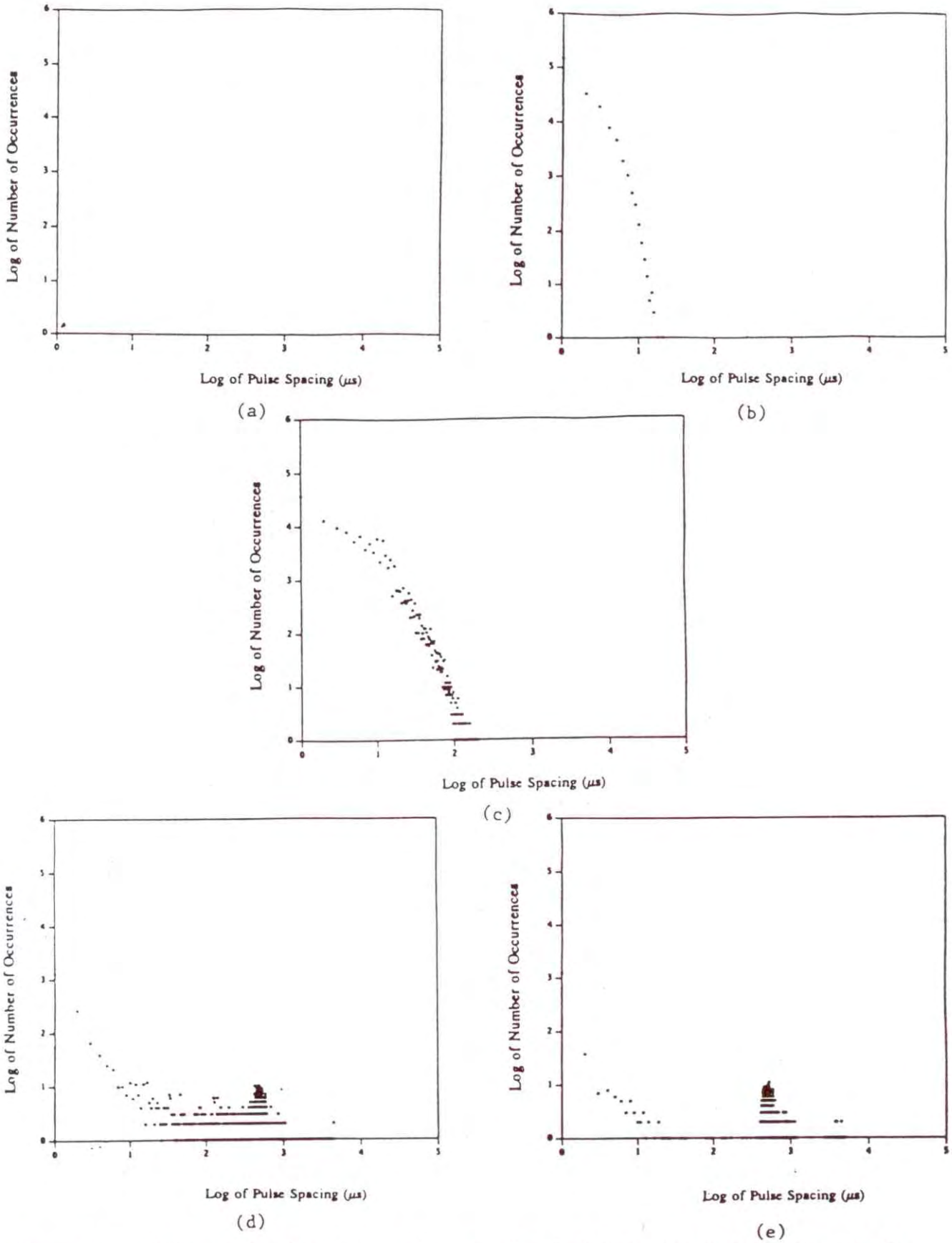


Figure 37. Pulse spacing distributions of measured noise/interference at thresholds of (a) 0, (b) 5, (c) 10, (d) 20, and (e) 30 (case study 5).

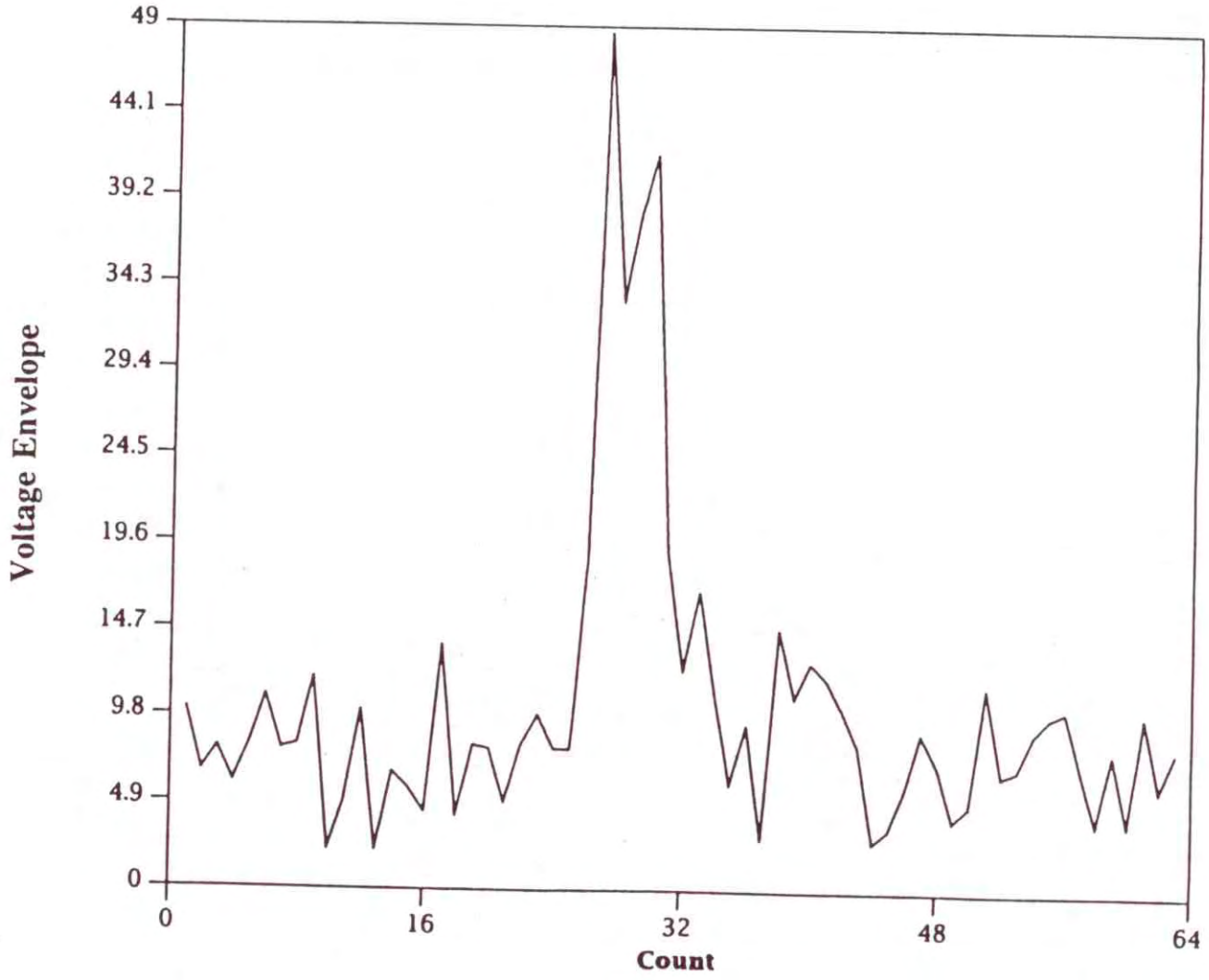


Figure 38. Voltage envelope of measured noise/interference on a scale from 0 to 64ms. (case study 5).

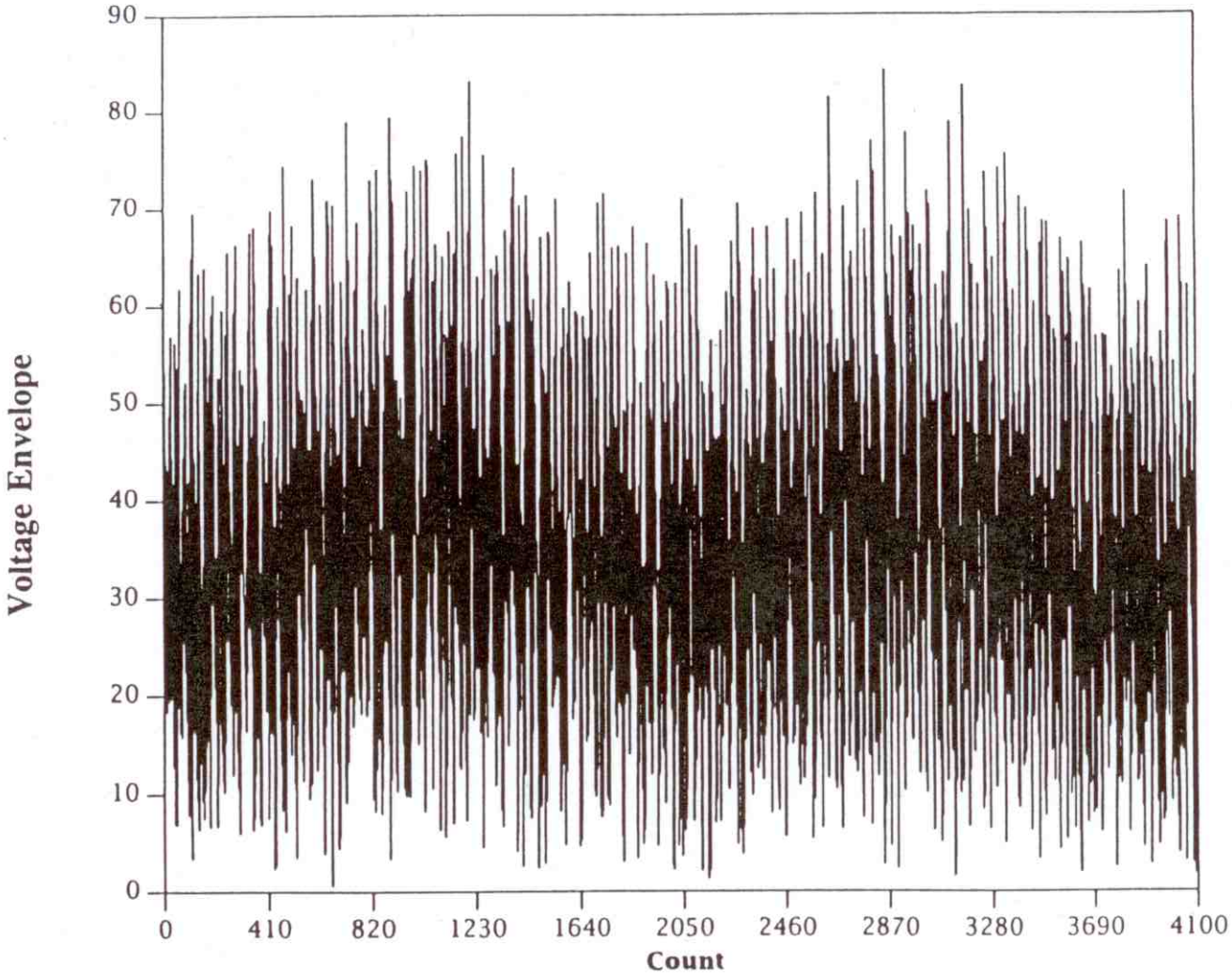


Figure 39. Voltage envelope of simulated noise/interference.

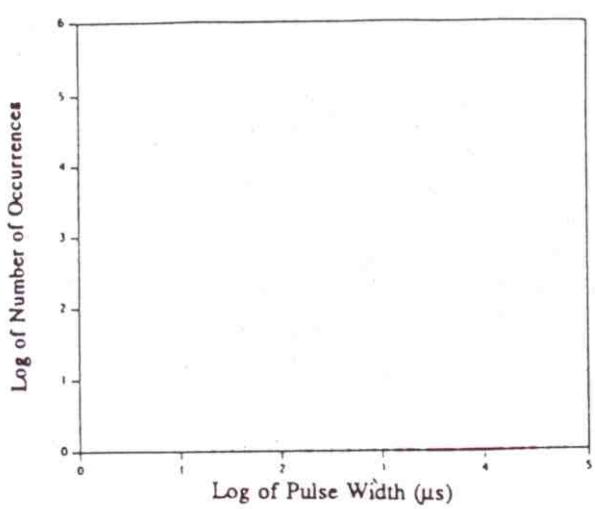


(a)

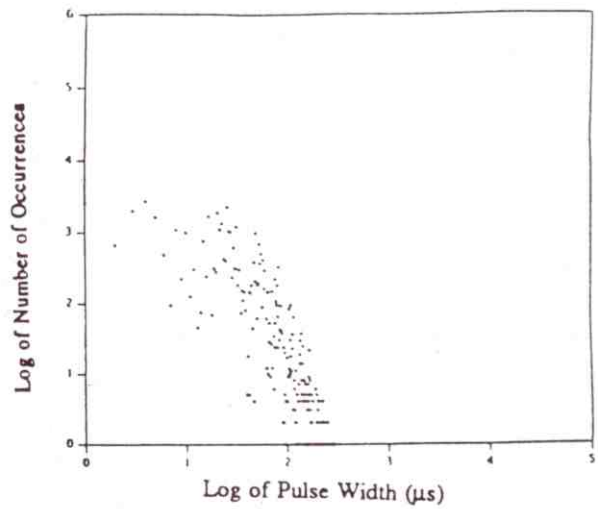


(b)

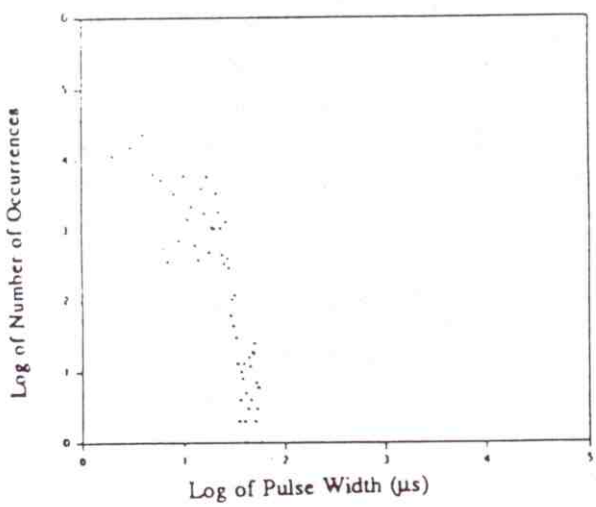


(c)

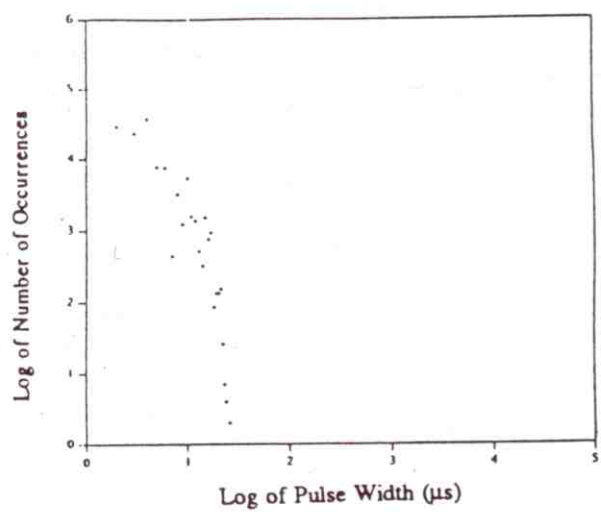


(d)

Figure 40. Pulse width distributions of simulated noise/interference at thresholds of (a) 0.5, (b) 10, (c) 20, (d) 30, (e) 40, (f) 50, (g) 70, and (h) 80.

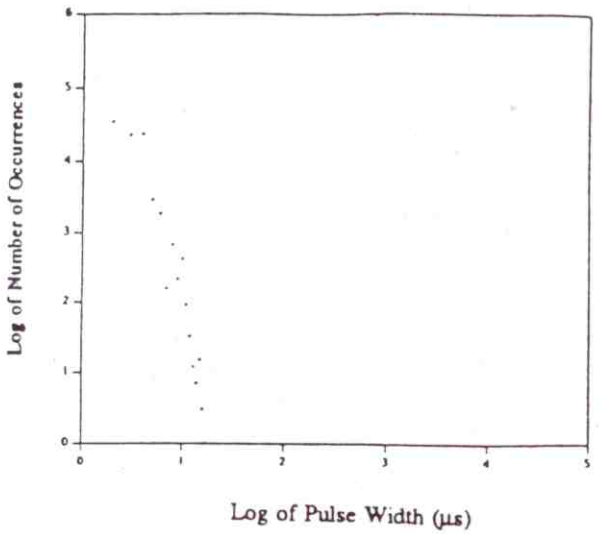


(e)

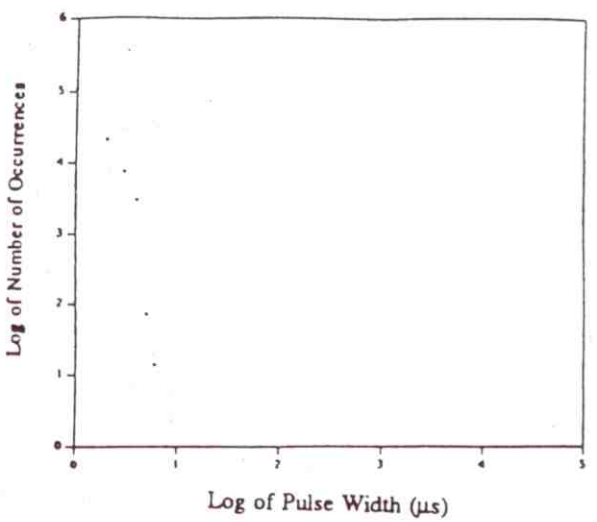


(f)

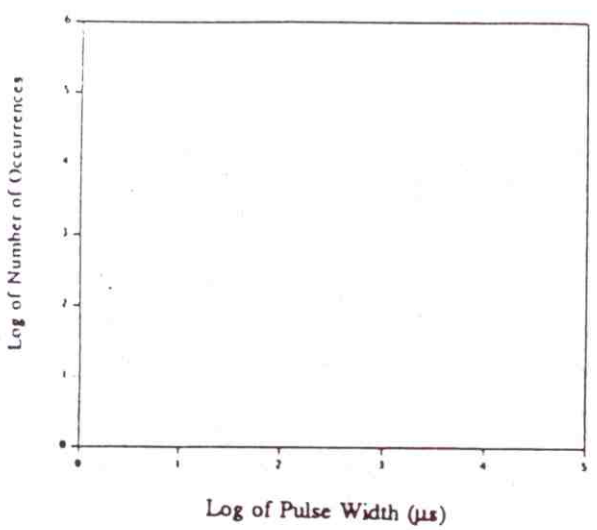


(g)

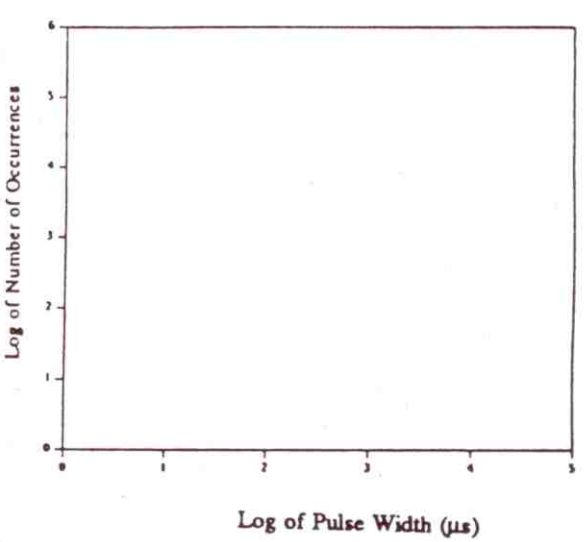


(h)

Figure 40 (cont.). Pulse width distributions of simulated noise/interference at thresholds of (a) 0.5, (b) 10, (c) 20, (d) 30, (e) 40, (f) 50, (g) 70, and (h) 80.

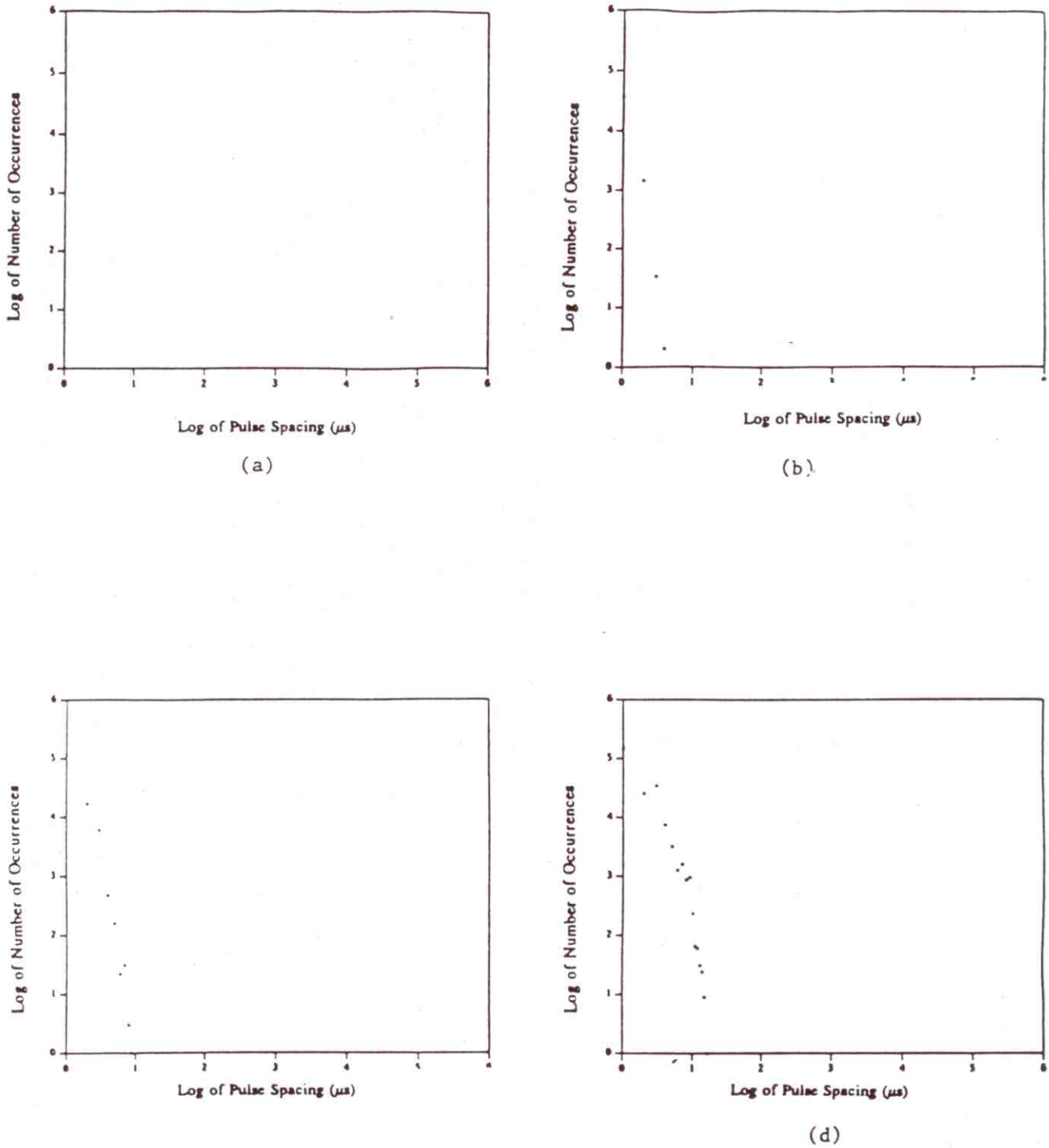


Figure 41. Pulse spacing distributions of simulated noise/interference at thresholds of (a) 0, (b) 10, (c) 20, (d) 30, (e) 40, (f) 50, (g) 70, and (h) 80.

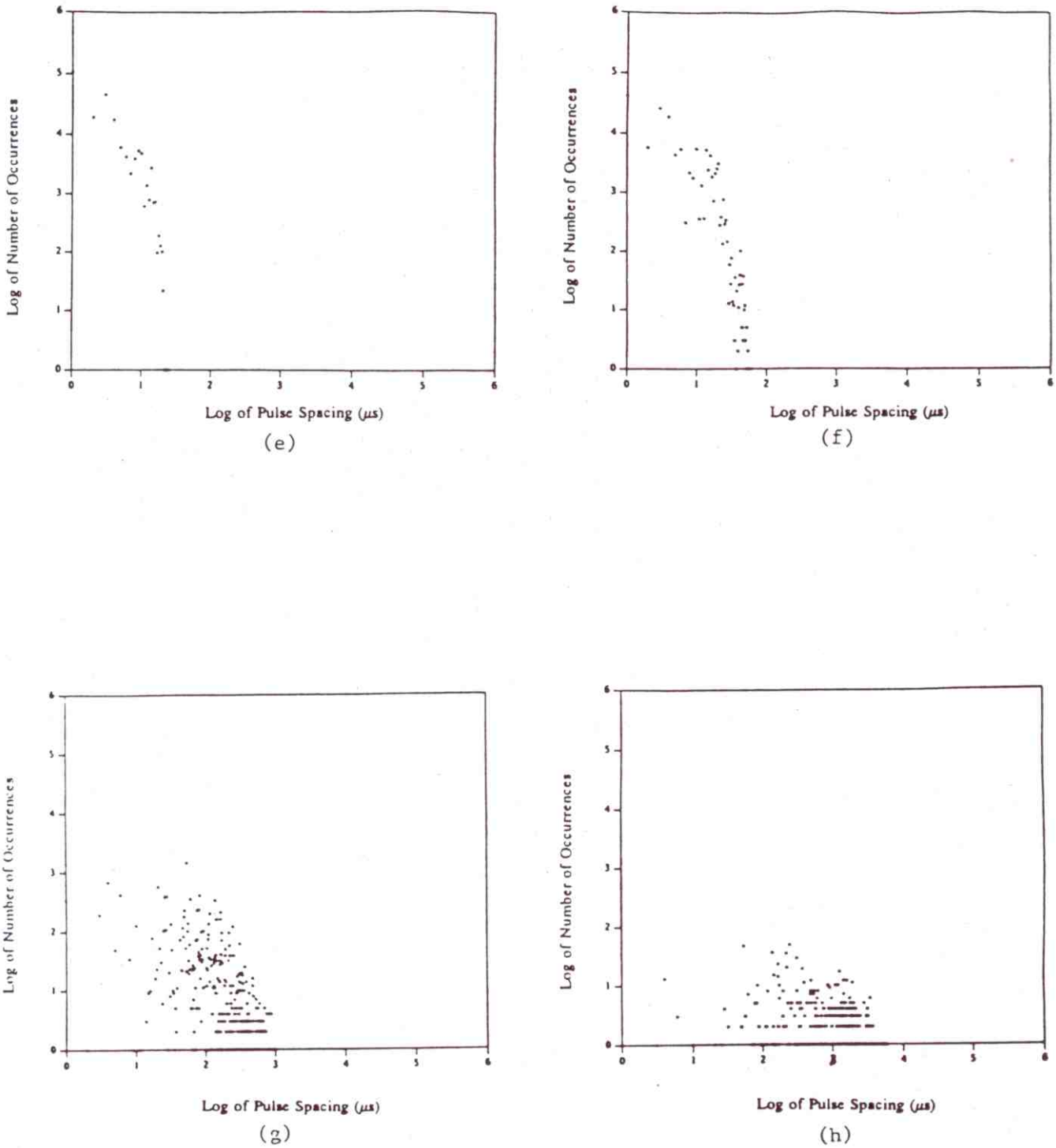


Figure 41 (cont.). Pulse spacing distributions of simulated noise/interference at thresholds of (a) 0, (b) 10, (c) 20, (d) 30, (e) 40, (f) 50, (g) 70, and (h) 80.

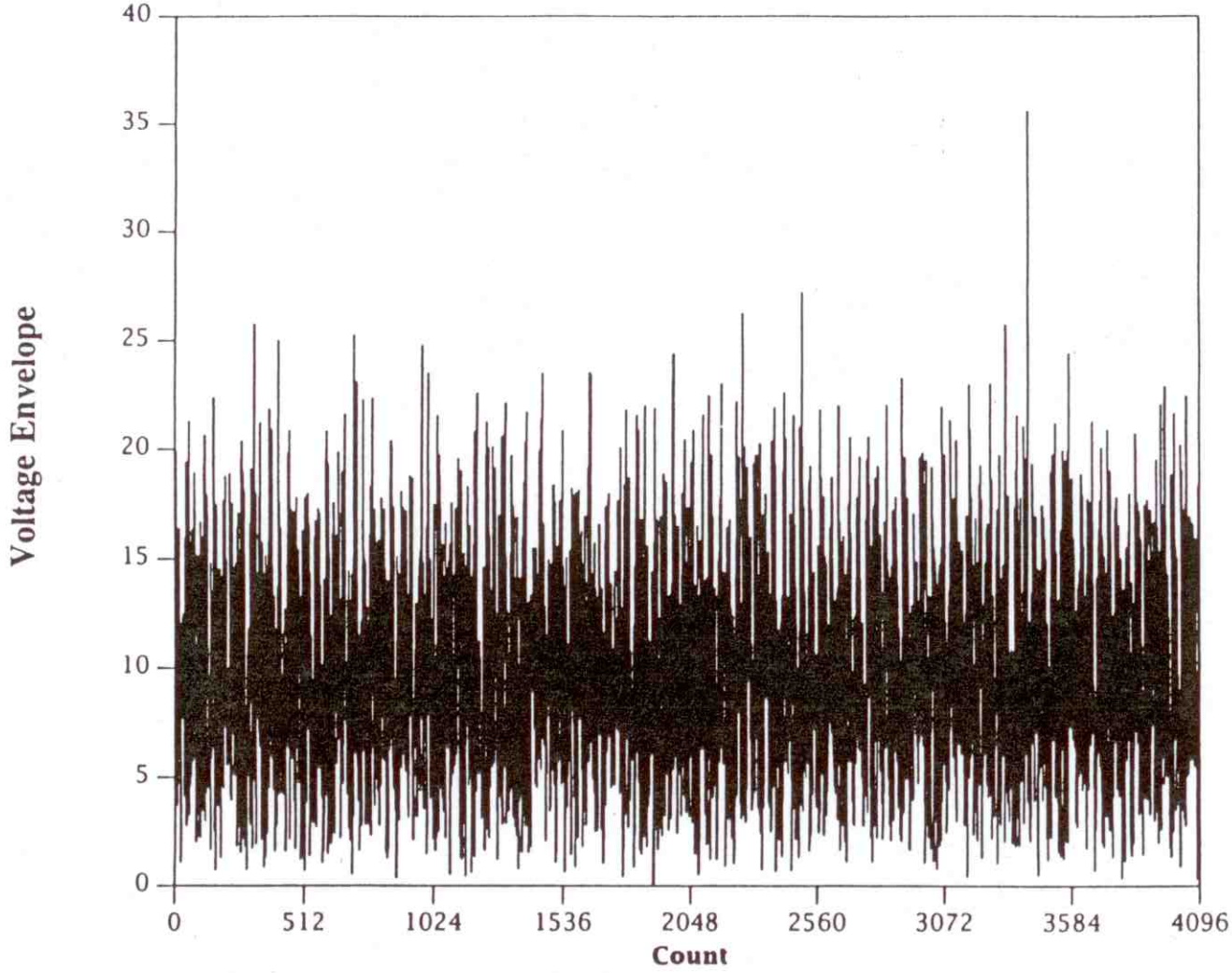


Figure 42. Voltage envelope of simulated noise/interference.

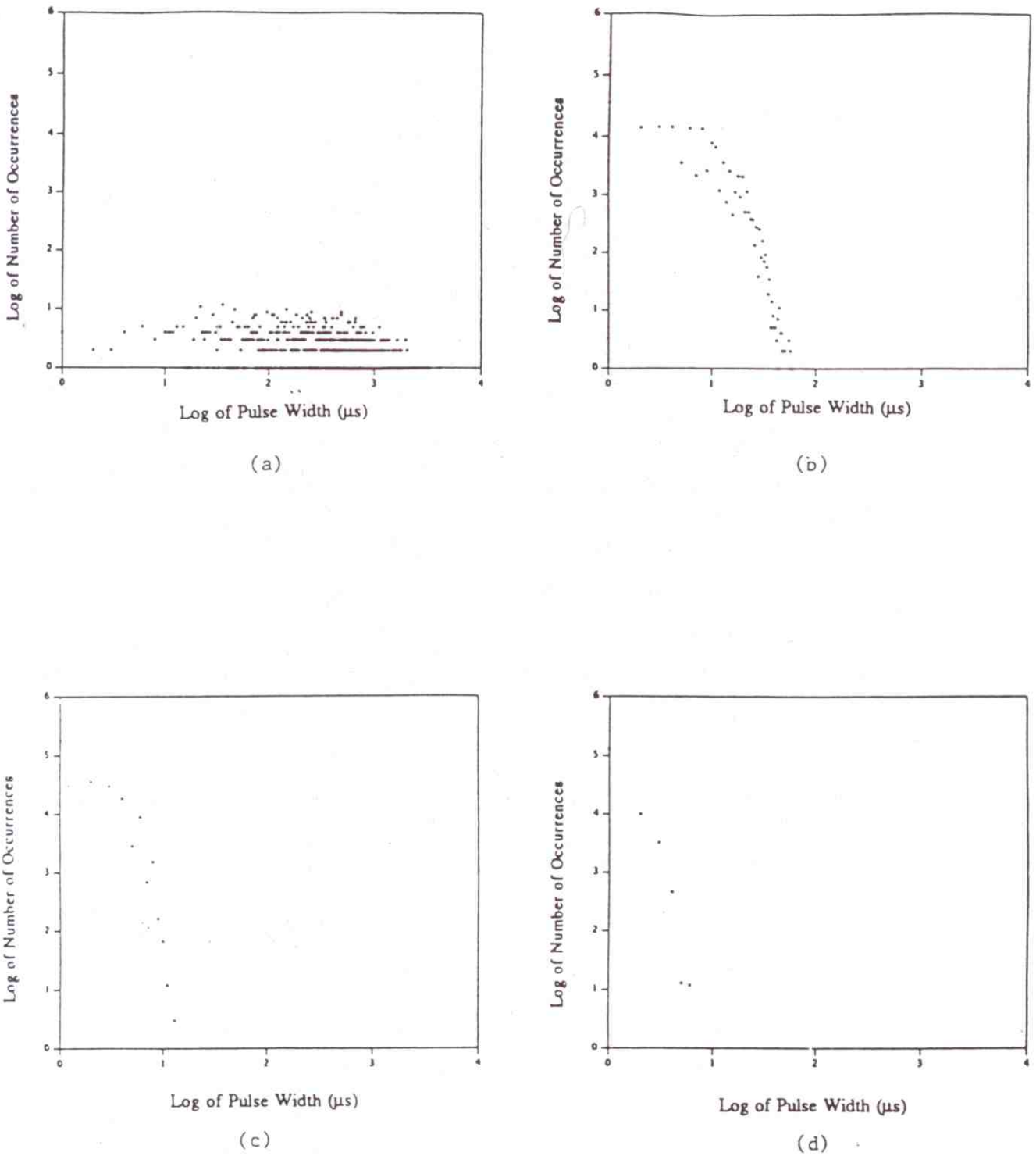


Figure 43. Pulse width distributions of simulated noise/interference at thresholds of (a) 0.5, (b) 5, (c) 10, (d) 15, (e) 20, (f) 25, (g) 30, and (h) 40.

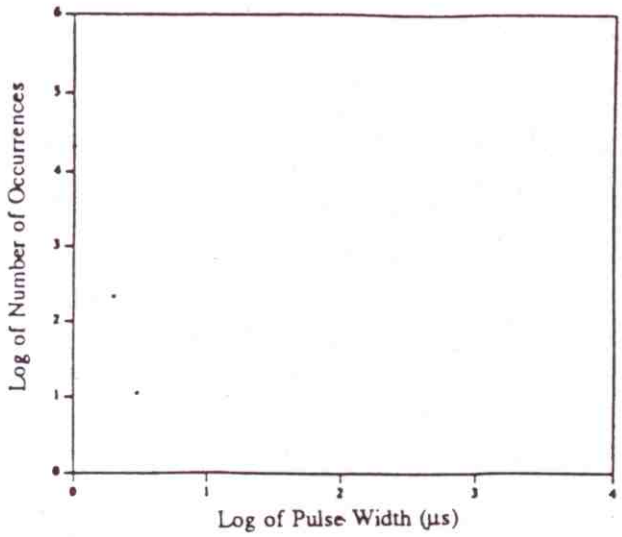


(e)

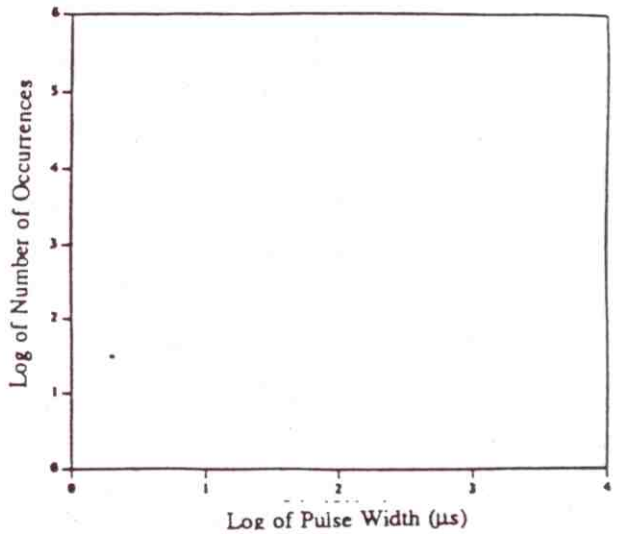


(f)

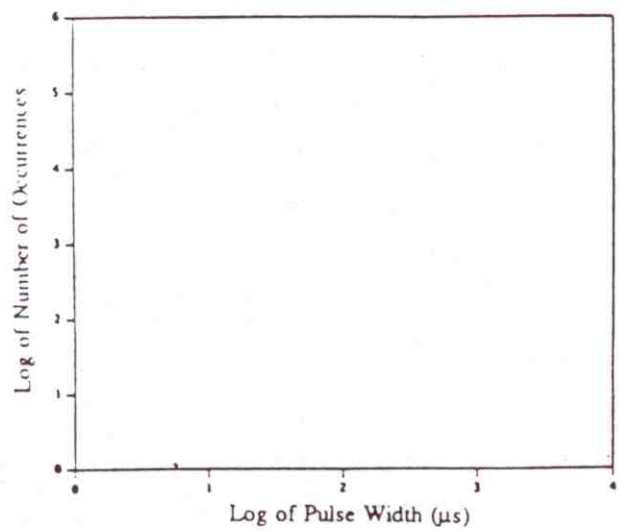


(g)

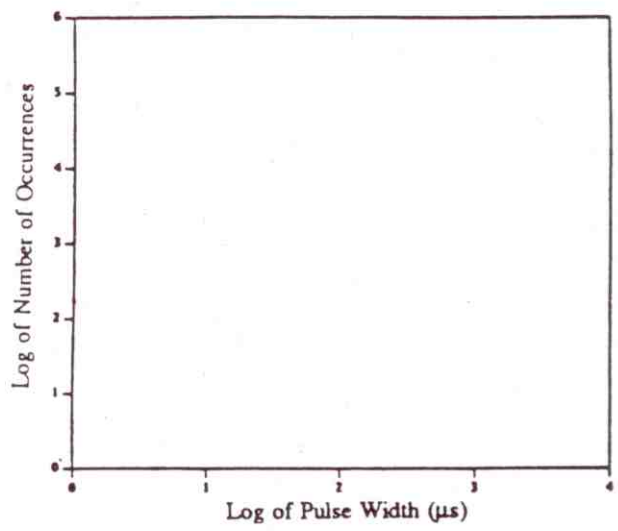


(h)

Figure 43 (cont.) Pulse width distributions of simulated noise/interference at thresholds of (a) 0.5, (b) 5, (c) 10, (d) 15, (e) 20, (f) 25, (g) 30, and (h) 40.

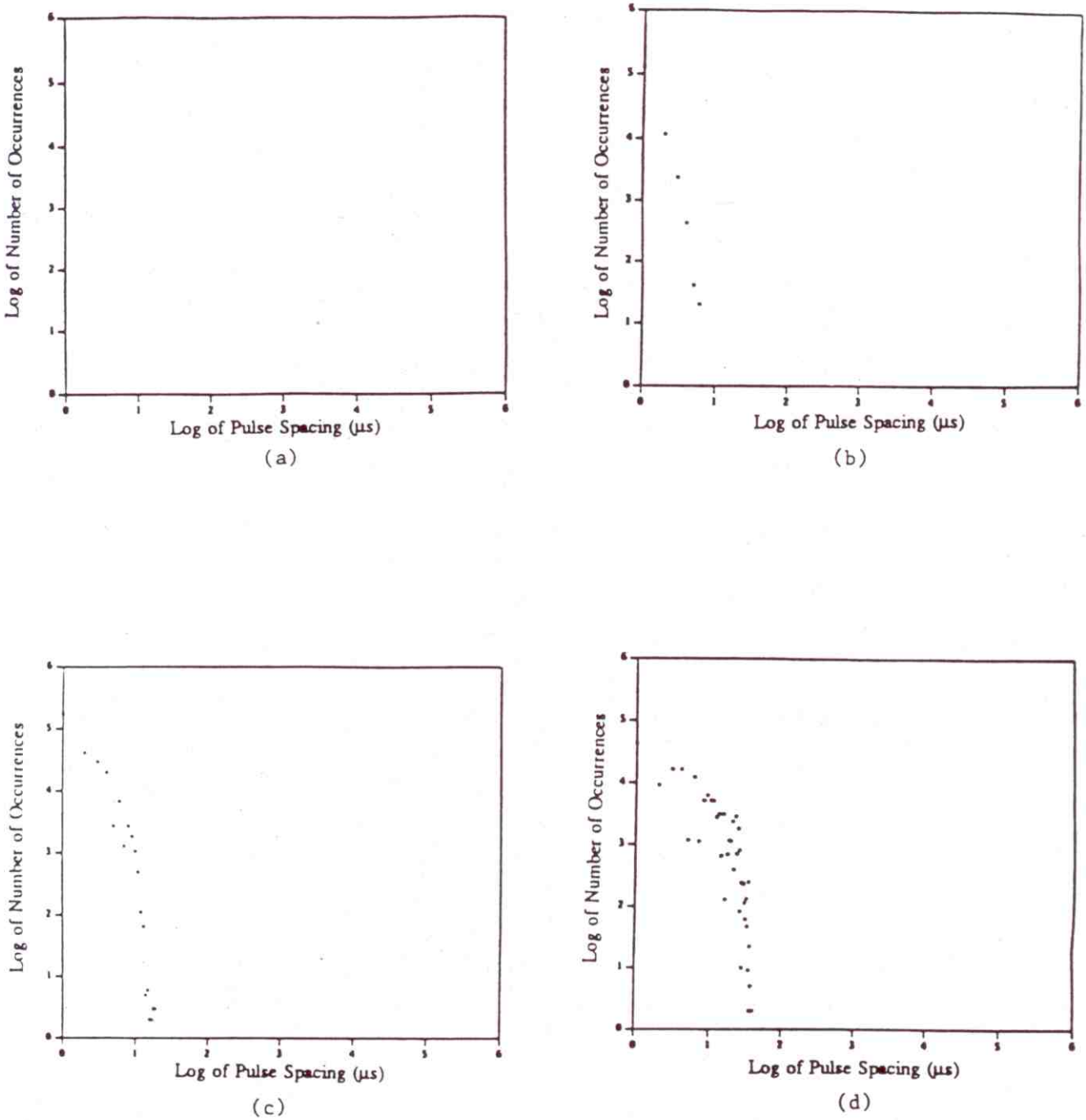


Figure 44. Pulse spacing distributions of simulated noise/interference at thresholds of (a) 0, (b) 5, (c) 10, (d) 15, (e) 20, (f) 25, (g) 30, and (h) 40.

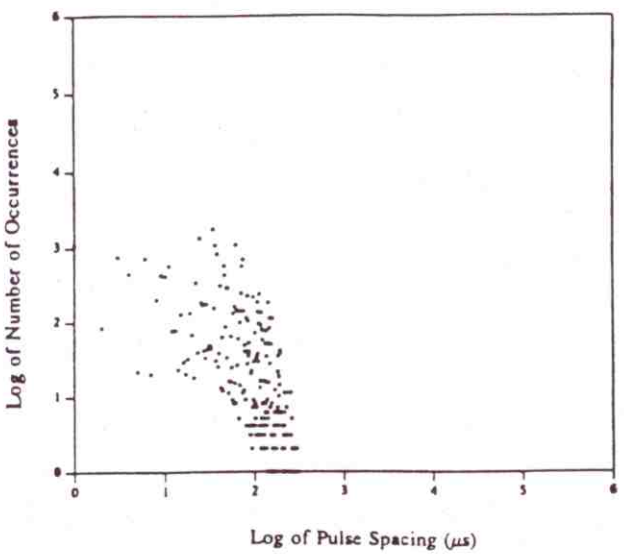


(e)

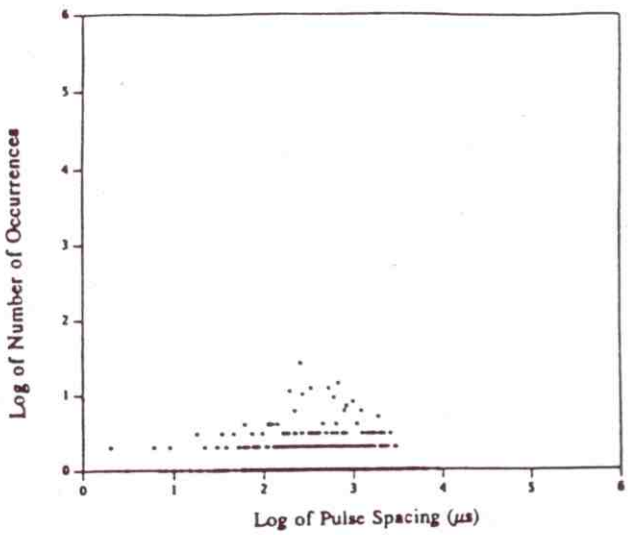


(f)

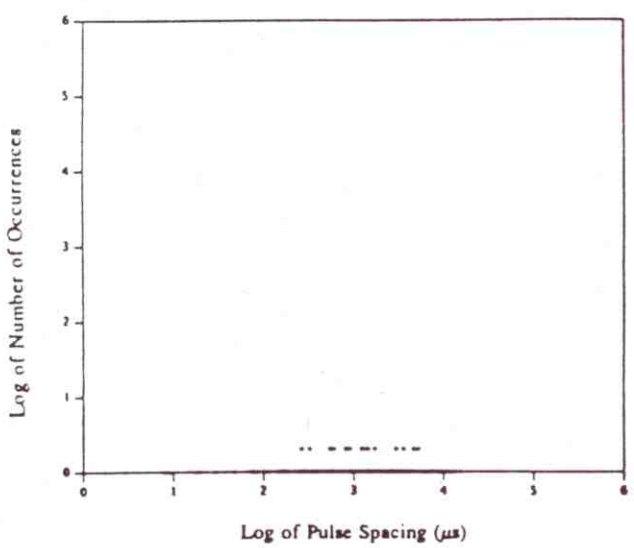


(g)

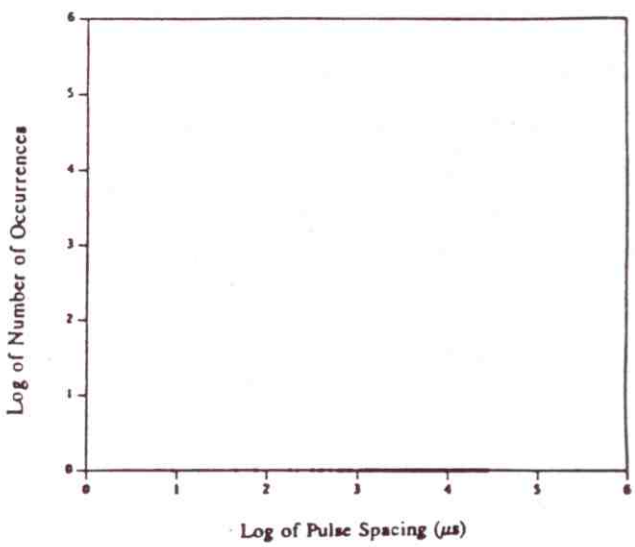


(h)

Figure 44 (cont.). Pulse spacing distributions of simulated noise/interference at thresholds of (a) 0, (b) 5, (c) 10, (d) 15, (e) 20, (f) 25, (g) 30, and (h) 40.

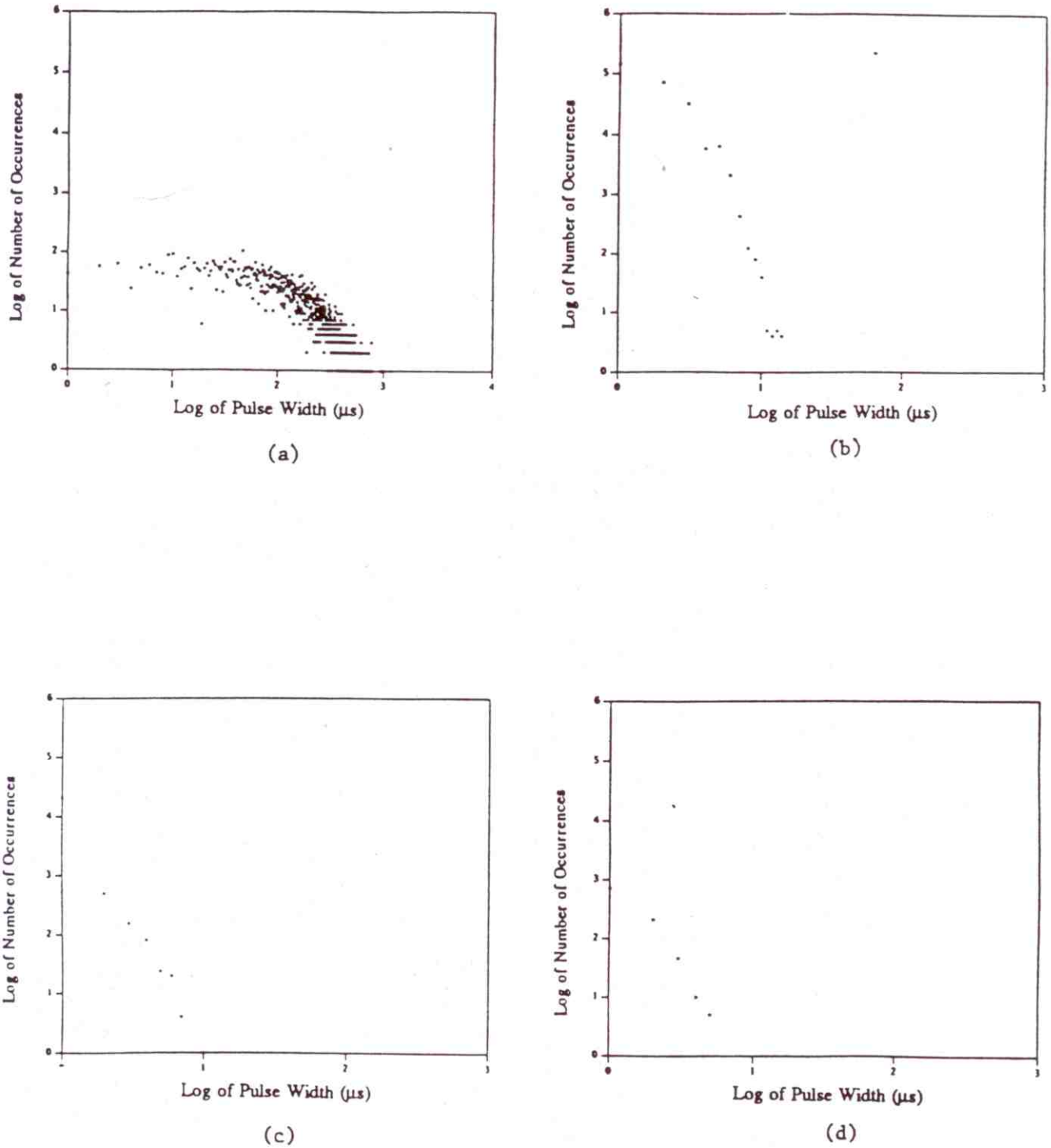


Figure 45. Pulse width distributions of simulated noise/interference at thresholds of (a) 0.5, (b) 5, (c) 10, (d) 15, (e) 20, (f) 25, (g) 30, and (h) 40.

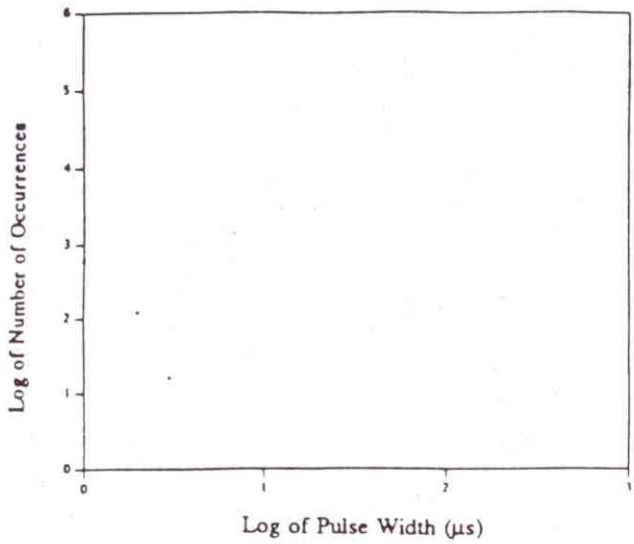


(e)

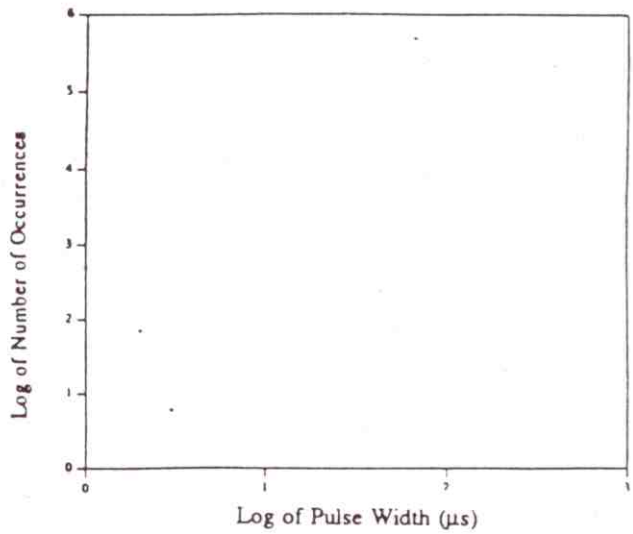


(f)

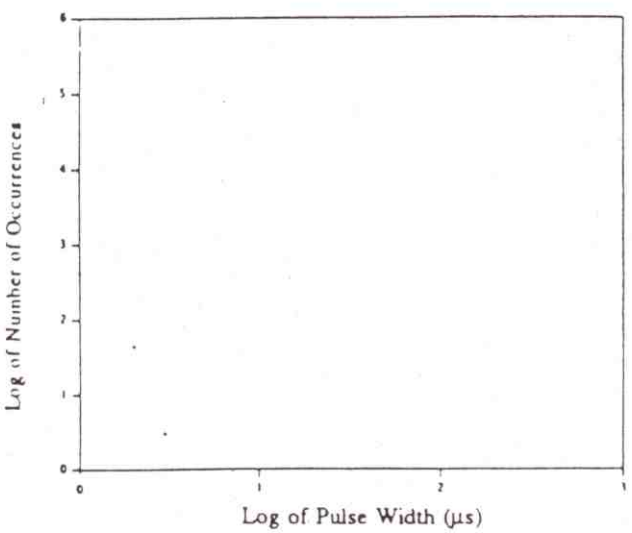


(g)

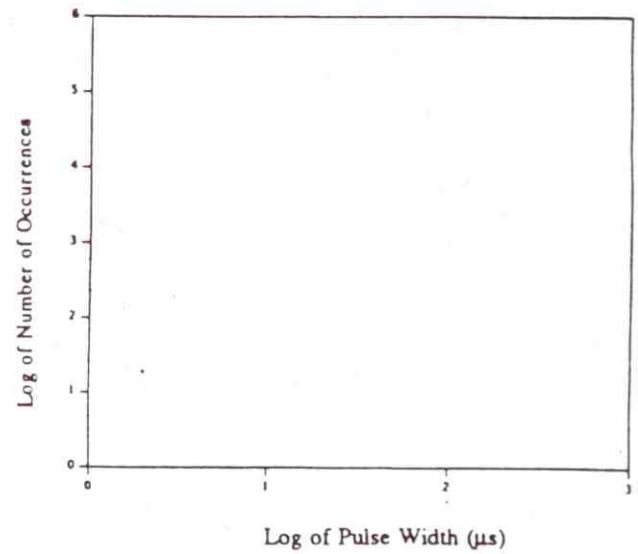


(h)

Figure 45 (cont.). Pulse width distributions of simulated noise/interference at thresholds of (a) 0.5, (b) 5, (c) 10, (d) 15, (e) 20, (f) 25, (g) 30, and (h) 40.

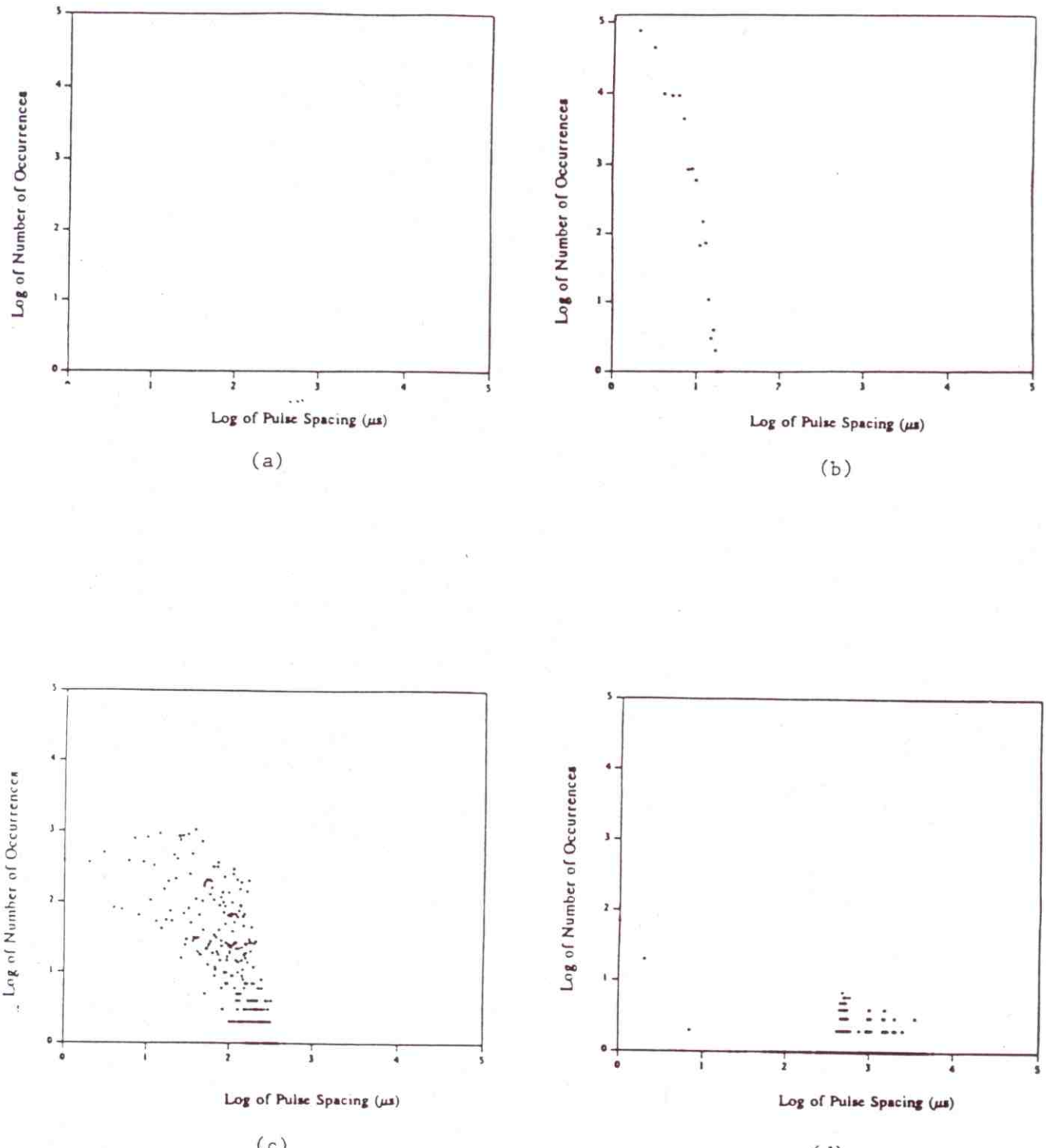


Figure 46. Pulse spacing distributions of simulated noise/interference at thresholds of (a) 0, (b) 5, (c) 10, (d) 15, (e) 20, (f) 25, (g) 30, and (h) 40.

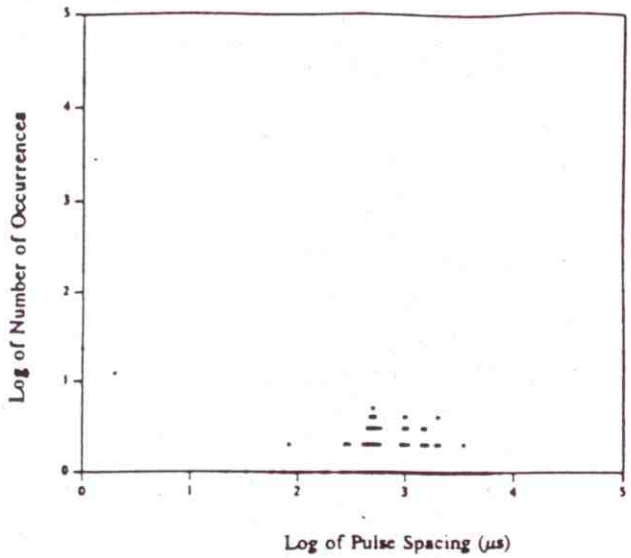


(e)

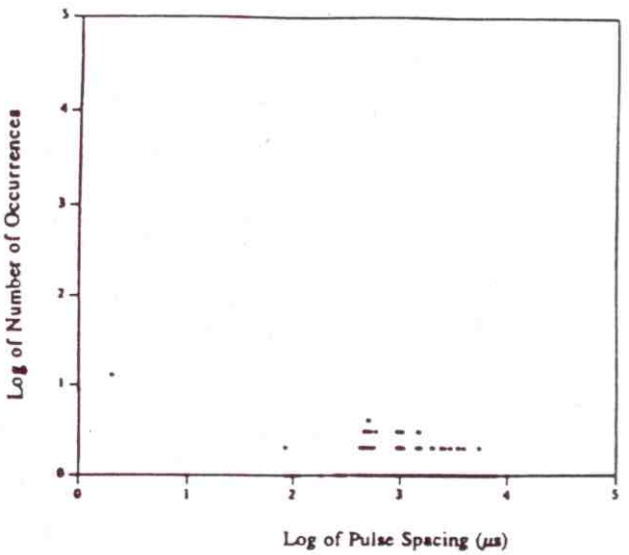


(f)

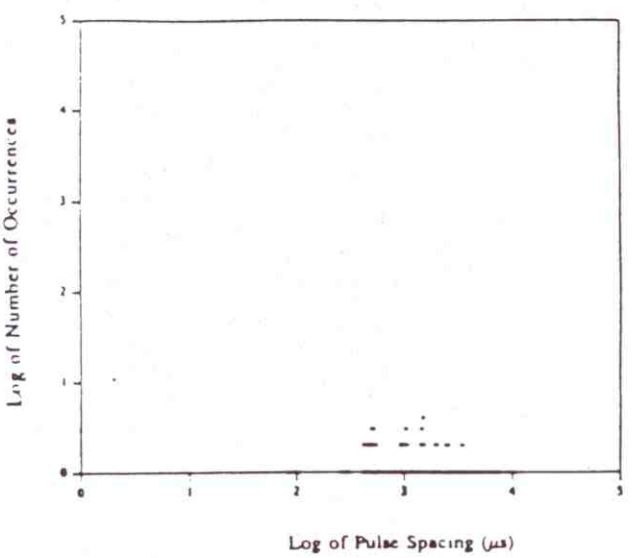


(g)

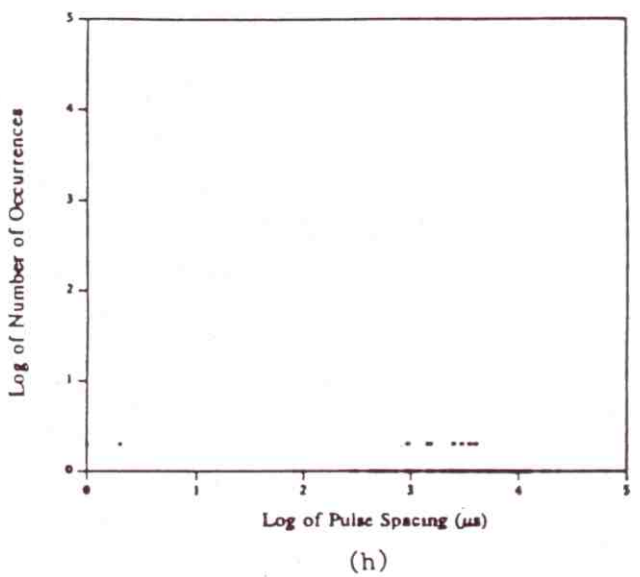


(h)

Figure 46 (cont.). Pulse spacing distributions of simulated noise/interference at thresholds of (a) 0, (b) 5, (c) 10, (d) 15, (e) 20, (f) 25, (g) 30, and (h) 40.

threshold one expects the pulse width distribution to have relatively few events, with those events occurring at relatively large widths. One also expects the pulse spacing distribution to have extremely few, if any, events, with such events occurring at the minimum spacing (1 μs).

As the threshold is gradually increased from zero, one expects to encounter upgoing and downgoing crossings more frequently, so that one expects the pulse width distribution to have relatively more events, with these events occurring at relatively smaller widths. Similarly, one expects the pulse spacing distribution to have numerous events (more than 0 or 1), with many of these events occurring at spacings greater than the minimum spacing (1 μs), because the probability that the envelope exceeds the threshold begins to decrease.

As the threshold is increased further and approaches the upper edge of the envelope, the probability that the envelope exceeds the threshold continues to decrease, and the number of envelope crossings is also decreasing. One therefore expects the pulse width distribution to have fewer events, with these events occurring at smaller widths. One also expects the pulse spacing distribution to have fewer events, with these events occurring at larger spacings.

Finally, to the extent that the upper and lower halves of the envelope are symmetric about the mean value of the envelope, one expects the pulse width and spacing distributions to exhibit complementary behavior in the following sense. Consider two values of the threshold which are symmetric about the mean value of the envelope; that is, the larger threshold exceeds the mean value of the envelope by the same amount that the smaller threshold is less than the mean value of the envelope. If the envelope is symmetric about its mean, one expects the distribution of upgoing crossings at the upper threshold to be identical to the distribution of downgoing crossings at the lower threshold, and vice versa. Thus, one expects the pulse spacing distribution at the upper threshold to be identical to the pulse width distribution at the lower threshold, and vice versa.

To varying degrees, all of these features are present in Figures 23 through 37. However, the pulse width and spacing distributions are especially helpful for modeling the impulsive noise in the fifth case study. For example, the pulse width distributions in Figure 36 at thresholds of 20 and 30 reveal numerous pulse widths between 2 and 10 μs, whereas the base width of the central lobe of an impulse filtered with a 400 kHz lowpass filter is 2.5 μs. A pulse width greater than 2.5 μs can be achieved either by passing an impulse through a filter with a bandpass less

of 2.5 μs, but whose times of arrival differ by less than 2.5 μs. However, the pulse spacing distributions in Figure 37 at thresholds of 20 and 30 reveal numerous pulse spacings on the order of or less than 10 μs, which is indicative of fine structure in the pulses, suggesting that the pulses consist of superpositions of individual impulses. That this is the case can be seen in Figure 38, which shows the voltage envelope for the fifth case study, plotted on an expanded scale between 0 and 64 μs. The pulse in the center of the plot consists of a superposition of two or more filtered impulses.

The pulse spacing distributions in Figure 37 at thresholds of 20 and 30 also exhibit bumps in the vicinity of 500 μs, which indicate that the pulses tend to occur periodically in time. However, the fact that the bumps have finite widths and are not delta functions indicates that the pulses are not precisely periodic, as discussed above. Thus, the level crossing distributions reveal both fine structure and time correlations associated with impulsive noise, which should be taken into account in the noise/interference model.

The level crossing distributions also indicate that the impulsive noise in the fifth case study is not atmospheric noise. Lightning flashes contain one or more strokes whose pulse widths are on the order of 100 microseconds, with spacings between strokes on the order of tens of milliseconds (Uman, 1987). On the other hand, the level crossing distributions for the fifth case study reveal pulse widths on the order of several microseconds and pulse spacings on the order of half a millisecond.

### 3.2 Comparisons of Model with Measurements

To investigate the level crossing properties of the noise/intterference model, simulations of one-second duration were performed, with and without impulsive noise. The noise/interference in the first simulation, to be compared with the first case study, consists of Gaussian noise and narrowband interferers, using the parameter values listed in Table 2. The first 4 ms of the voltage envelope are plotted in Figure 39, and the pulse width and pulse spacing distributions computed from the entire one-second record are shown in Figures 40 and 41, respectively.

The pulse width distribution at zero threshold has not been displayed in Figure 40 because there are no occurrences of pulse widths at this threshold; as explained above, the occurrence

of one or more events would require the I- and Q-channel voltages to simultaneously vanish at two or more sample times, which is extremely unlikely. On the other hand, the pulse width distributions of the measured data at zero threshold show numerous occurrences. This is because the data were obtained using A/D converters with a finite resolution (finite number of bits). Thus, values of the voltage envelope which are finite, but less than the resolution of the A/D converters, are recorded as zero. Therefore, to make a meaningful comparison between the measured and simulated distributions at small values of the threshold, the simulated distribution has been computed for a small, but finite (0.5) value of the threshold. Aside from this caveat, the general characteristics of the distributions computed from the measured data in the first case study (Figures 24 and 25) and the simulated data appear very similar to one another.

The noise/interference in the second simulation, to be compared with the fifth case study, consists of Gaussian noise, narrowband interferers, and impulsive noise using the parameter values listed in Table 3. The impulses are uniformly distributed in time; that is, 50 impulses are uniformly distributed in time within each 4 ms block of the simulation, resulting in a total of 12,500 impulses in the entire one-second simulation. The first 4 ms of the voltage envelope are plotted in Figure 42, and the pulse width and pulse spacing distributions computed from the entire one-second record are shown in Figures 43 and 44, respectively. At the lower values of the threshold (less than 20), the measured (Figures 36 and 37) and simulated distributions are qualitatively similar. However, at the higher thresholds the pulse widths of the simulated data are narrower than those of the measured data. The simulated pulse spacing distributions also fail to reproduce the features of the measured distributions. For example, at a threshold of 30 the simulated distribution does not have the pronounced tail that the measured distribution has at small pulse spacings, and the bump in the simulated distribution in the vicinity of 500-1000 μs is much broader than it is in the measured distribution. This is not unexpected, since no attempt was made to model the fine structure of the pulses by superimposing filtered impulses, and the impulses were not correlated in time, but were uniformly distributed in time (within each 4 ms block).

To rectify these deficiencies, noise/interference was simulated using the same parameter values that were used in the previous example, but with the impulses correlated in time using the following procedure. First, the impulses are distributed only within windows of 4 μs duration.

The window that each impulse is placed within is chosen randomly from the total set of windows, and within each window the distribution of arrival times is uniform. Second, the spacing between the centers of the windows is a random variable uniformly distributed between 450 μs and 550 μs. Thus, the impulses occur in bursts which exhibit fine structure (with an average of 6.25 impulses per burst), and the arrival times of the bursts are approximately (but not precisely) periodic. As in the previous simulation, 50 impulses are distributed within each 4 ms block, resulting in a total of 12,500 impulses in the entire one-second simulation.

The resulting pulse width and pulse spacing distributions are shown in Figures 45 and 46, respectively. The distributions in Figure 45 indicate that, relative to the previous example, the pulse widths at high thresholds have been broadened (due to the superposition of filtered impulses within the bursts). Also, the pulse spacing distributions at high thresholds in Figure 46 have a tail at small values of pulse spacing (due to the fine structure within the bursts), and the bump in the vicinity of 500-1000 μs is narrower than in the previous example (due to the time correlations of the bursts). Although the simulated distributions typically have fewer occurrences associated with these features than do the measured distributions, these differences in the number of occurrences could be removed by simulating the impulsive noise with a greater number of impulses. One could also envisage a more sophisticated modeling of the arrival time distribution of the impulses to more accurately reproduce the shapes of these features. However, the examples demonstrate that the qualitative features in the measured distributions that cannot be simulated using uniformly distributed times of arrival of the impulses can be simulated by appropriately distributing the impulses in time.